1967

The magnetic characteristics of electrodeposited nickel-phosphorus

Jim Riley Goodin
Lehigh University

THE MAGNETIC CHARACTERISTICS OF ELECTRODEPOSITED NICKEL-PHOSPHORUS

by

Jim R. Goodin

A Thesis

Presented to the Graduate Faculty

of Lehigh University

In Candidacy for the Degree of

Master of Science

Department of Metallurgy and Materials Science

Lehigh University

1967

CERTIFICATE OF APPROVAL

This thesis is accepted and approved in partial fulfillment of the requirements for the degree of Master of Science.

17 May 1967
Date

George P. Cernard III
Professor in Charge

T. J. Lubinski
Chairman of the Department
of Metallurgy and Materials Science

ACKNOWLEDGEMENTS

The author wishes to express his sincere appreciation to the following who also have made a significant contribution to this thesis:

To Dr. G. P. Conard for protecting me from the errors of omission and commission as well as providing invaluable suggestions.

To Mr. A. J. Avila for direction and for the existence of his group and professional staff in which I worked.

To Messrs. S. J. Borcsik, T. J. Dewees, and R. E. Thomas for laboratory assistance.

To Mr. S. J. Buzash for advice and assistance on metallography.

To others too numerous to mention.

To Lehigh University and the Western Electric Co. for this opportunity.

TABLE OF CONTENTS

TABLE OF CONTENTS (cont'd)

LIST OF FIGURES

LIST OF FIGURES (cont'd)

LIST OF FIGURES (cont'd)

LIST OF TABLES

ABSTRACT

The electrodeposited system nickel-phosphorus up to 15 w/o P is examined for magnetic behavior as influenced by composition and structure. This behavior is related to the electrolessly plated Ni-P system by analogy. A structure analysis is made using x-ray and metallographic techniques. Magnetic measurements are made using an AC hysteresis loop tracer. An analysis is presented of the effect of heat treatment. The magnetic characteristics of as-plated alloys are explained by considering the effect which alloying has on the Curie temperature and by adapting fine particle theory. The magnetic characteristics of heat treated alloys are explained with fine particle theory alone.

I. INTRODUCTION

The electrodeposition of phosphorus with nickel is of academic interest in that phosphorus is nonmetallic and is deposited from an anion with the resulting alloys being quite sound and having good metallic properties. Phosphorus is one of the few, if not the only, nonmetals exhibiting this phenomenon. Of practical interest is the fact that these alloys represent the form which nickel takes when it is deposited by chemical reduction or as it is more commonly known, electroless plating.

The deposition of phosphorus with nickel in electroless plating is a necessary "evil" due to the chemical nature of the process rather than by choice. The range is usually 6 - 10 w/o (weight per cent) phosphorus with little concern as to the actual amount just so long as the plate is acceptable. In electrodeposition, however, the phosphorus is present by choice and produces certain desirable characteristics in the deposits such as more brightness and increased hardness over pure nickel. Here the phosphorus content ranges from zero to an approximate maximum of 15% which permits a greater latitude of properties. However, the deposits tend to be brittle and highly stressed. Because of this, electrodeposition of nickel-phosphorus is not of too widespread use and electroless nickel is by far the more important of the two. Furthermore, it can be deposited on any properly activated surface such as plastic or glass and has excellent covering power.

In spite of the greater importance of electroless nickel, electrodeposition was chosen for the preparation of the alloys in this

investigation because of the lack of precise and consistent control over composition plus the relatively limited w/o P range obtainable with the former method. Investigations which have been conducted to date have shown that nickel-phosphorus obtained by either chemical reduction or electrodeposition has identical physical and mechanical properties depending solely on the w/o phosphorus[1]. Therefore we should be justified in relating whatever conclusions are drawn in this paper to alloys obtained by either means, although this is admittedly a point of conjecture when considering magnetic characteristics where prior correlation is limited.

Because of the extensive use of electrolessly plated nickel, several recent investigations of its mechanical and physical properties have been made. Magnetic properties of this system as well as the electrodeposited system have not been as thoroughly investigated. Available information is limited to a qualitative description of the reaction of Ni-P films to a magnet plus an observation of the complete attenuation of ferromagnetic behavior at an approximate minimum phosphorus content[2,3]. Consensus is that alloys of greater than 8 w/o P are paramagnetic with those of less P having diminishing magnetic properties with decreasing Ni content. Regardless of the method of preparation, a thorough understanding of the magnetic characteristics of Ni-P alloys is lacking.

There is little information to be found in the literature on the magnetic properties of pure nickel and nickel-rich alloys obtained by electrodeposition. The primary reason for this is that the coercivity of nickel obtained in this manner, which is in the range

20-100 Oe (oersteds), has no immediate commercial significance. Magnetic materials of 200 plus Oe are used in permanent memory devices and those with high permeability and less than 20 Oe coercive force find use in other applications. Koretsky[4] states without elaboration that Ni-P films which are paramagnetic as-plated, can be rendered highly ferromagnetic with extremely square loops and coercivity of 250 plus Oe by annealing at 400°C for 30 minutes in dry nitrogen. This would yield Ni-P films which were ferromagnetic to the order of commercial significance, however Koretsky indicates a detrimental aging tendency reducing the coercivity to some 180 Oe.

The annealing temperature given above of 400°C is also the heat treat temperature which produces the maximum degree of hardness in the alloys. This is reported to involve a precipitation hardening reaction[5] producing a dispersion of Ni_3P in Ni or vice versa[6,7]. This latter point has not been agreed upon. From the generally accepted theory of precipitation hardening the conclusion could be drawn that the as-plated material is crystalline, but most investigators have found from x-ray studies that the structure is amorphous[8]. Their conclusion was based on x-ray Laue pinhole photographs having, instead of Debye rings, a single halo which is characteristic of amorphous materials. Graham[9], however, used electron diffraction techniques to show the material is actually a supersaturated solid solution of phosphorus in crystalline nickel and explained the previous results as due to the effect of extremely fine grain size. Phosphorus is known to refine grain size in

electroplated nickel.

Considering the fact that the maximum phosphorus obtainable by either of the two methods under discussion should be less than 15 w/o, the Ni-P phase diagram shown in Figure 1[10] shows that only a simple two phase reaction between Ni and Ni_3P should be involved. Also, the optimum heat treatment temperatures of 400-450°C are well within the lower left two phase region of the diagram. Therefore the magnetic properties after heat treatment will be a function of the magnetic character of Ni, Ni_3P and any non-equilibrium phases which might be formed. Unfortunately, no information is available on this point for the compound Ni_3P, but it is known that the analogous Fe_3P is ferromagnetic at room temperature as are the following: Fe_2P, MnP, Co_2P, Co_5As_2, Mn_3As_2, Mn_5P_2[11].

All the phosphides shown on the phase diagram, plus others, have been variously reported in the literature[12] but Graham[13] found no evidence for any other than Ni_3P. It can be seen in Figure 1 that the solid solubility of phosphorus is not given; nor is it known. Consensus is that it is extremely low.

A group of Russian investigators correlated the absence of ferromagnetism in as-plated electrolessly obtained alloys with the amorphous structure and noted that heat treatment produced crystallinity and ferromagnetism[15]. The problem was not investigated in depth, however.

From these, hopefully, interrelated points, the purpose of this investigation was evolved as follows:

(1) To correlate the composition of the alloys with the mag-

netic characteristics as-plated, after heat treating and after aging with consideration given to remanent magnetization, saturation magnetization, hysteresis loop squareness and primarily, intrinsic coercive force.

(2) To establish the structure as-plated and after heat treating using x-ray and metallographic techniques.

(3) To compare the structure to that dictated by the phase diagram.

(4) Finally, to propose a theory for the magnetic behavior in terms of the composition and structure.

II. EXPERIMENTAL PROCEDURE

A. Electrodeposition

1. Baths

The composition and operating parameters of the electrodeposition baths are as shown in Table 1.

TABLE 1

Hi-Phosphorus Bath

Constituent	Concentration
Nickel Sulphate - $NiSO_4 \cdot 6H_2O$	150 g/l
Nickel Chloride - $NiCl_2 \cdot 6H_2O$	50 g/l
Phosphorous Acid - H_3PO_3	40 g/l (116 ml of 30%)
Phosphoric Acid - H_3PO_4	adjust bath to pH 1.0

Parameter	Value
Temperature	80°C
Anode to Cathode Ratio	2:1
Current Density	10-20 amps/decimeter^2

Med-Phosphorus Bath

Constituent	Concentration
Nickel Sulphate - $NiSO_4 \cdot 6H_2O$	150 g/l
Nickel Chloride - $NiCl_2 \cdot 6H_2O$	50 g/l
Phosphorous Acid - H_3PO_3	10 g/l (29 ml of 30%)
Phosphoric Acid - H_3PO_4	adjust bath to pH 1.0

Parameter	Value
Temperature	$80^{o}C$
Anode to Cathode Ratio	2:1
Current Density	10-40 amps/dm^2

Lo-Phosphorus Bath

Constituent	Concentration
Nickel Sulphate - $NiSO_4 \cdot 6H_2O$	150 g/l
Nickel Chloride - $NiCl_2 \cdot 6H_2O$	50 g/l
Phosphorous Acid - H_3PO_3	1.75 g/l (5 ml of 30%)
Phosphoric Acid	adjust bath to pH 1.0

Parameter	Value
Temperature	$60^{o}C$
Anode to Cathode Ratio	2:1
Current Density	2-20 amps/dm^2

Min-Phosphorus Bath

Constituent	Concentration
Nickel Sulphate-$NiSO_4 \cdot 6H_2O$	120 g/l
Nickel Chloride-$NiCl_2 \cdot 6H_2O$	39 g/l
Phosphorous Acid - H_3PO_3	20 g/l (60 ml of 30%)
Phosphoric Acid - H_3PO_4	75 ml
Nickel Carbonate - $NiCO_3$	adjust bath to pH 1.0

Parameter	Value
Temperature	50-70-90°C
Anode to Cathode Ratio	2:1
Current Density	8 amps/dm^2

Each bath was prepared from reagent grade chemicals and deionized water. The baths were then electrolytically purified and equilibrated (commonly known as dummying) by plating on a sacrificial copper cathode at low current density (2 amps/dm^2) for one hour. This technique is used to remove and/or decompose impurities. In addition, experience has shown that the initial plating from a new bath tends to be inconsistent in properties. The low current density used results in a negligible removal of desired constituents from the baths.

2. Anode

The anode used was a 1/16" thick plate of rolled, depolarized high purity nickel (99.8%). The other dimensions were cut to size to produce a surface area of 50 cm^2 to maintain the correct anode to cathode ratio of 2:1 using the cathode described later. All anodes were analyzed as described under section F.2 following. During deposition, the anode was enclosed in a nylon bag used to retain nickel oxide sludge and fine nickel particles which will roughen the deposit unless checked.

3. Cathode

3.1 Material

Two cathodes were used. One was dead soft, high purity

99.99% copper coupons of 0.008" x 2" x 3" dimensions. This cathode was used only for the metallographic work described in section G. following, due to the need for a support for the samples during mounting, polishing, etc. For all other studies it was desired to remove the substrate from the sample so as to preclude any extraneous effect it might have in the subsequent phases of the investigation. With this in mind a thin, 0.001" thick foil of OFHC 99.999% copper was selected. All cathode material was analyzed as described under section F.2 following.

3.2 Preparation

The substrates were prepared for electrodeposition in the following manner:

A. Swabbed with trichlorethylene.

B. Hot air dried.

C. 15 sec. immersion in 2 parts H_2SO_4
1 part HNO_3
5 parts H_2O.

D. Water rinse.

E. Hot air dried.

The cleaned substrates were used immediately or stored in a dessicator.

Prior to use the cathodes were masked with 3M electroplating tape so as to produce a sample of the desired dimensions. It was found convenient to have a final surface area on the front of the cathode of 25 cm^2 or 0.25 dm^2. This permitted easy and consistent regulation of the current density. For instance, application of 2.5

amps current produced exactly 10 amps/decimeter^2 current density. A single area of 4.15 ± 0.05 cm x 6 cm was used on the coupons. For the foil, other considerations were necessary. The coupons were sufficiently rigid due to their thickness, but the foil required a support to prevent curling during deposition. A rigid fiberboard was used which was completely protected from the solution by electroplating tape. The foil, as can be seen in a prepared cathode in Figure 2, was masked off into six sections, each of 2.05 ± 0.05 cm square which proved to be a convenient dimension for the samples. This achieved an estimated 25.0 ± 0.5 cm^2 in six dimensionally and compositionally uniform samples per run. A solid area equal to that of the coupons was tried first but it was found that the deposit was not uniform due to current density variation. This was noted as an increase in thickness at the edges of the plate. Since deposition of phosphorus is sensitive to current density this was highly undesirable. The problem was seen to be corrected by the technique employed.

3.3 Removal

After the deposition on the foil was completed, the tape was removed, excess copper trimmed away with scissors, and the remaining copper stripped from the sample by immersion in a solution of the following composition:

Chromium Trioxide	- CrO_3	150 g
Sulfuric Acid	- H_2SO_4	8 ml
H_2O		500 ml

5 to 15 minutes at 60°C was required for complete removal. This solution has been shown to have negligible effect upon the nickel-

phosphorus alloy[16] and none was noted. After stripping, the samples were rinsed thoroughly in deionized water, hot air dried and stored in a dessicator.

4. Equipment

The plating current source was a Rapid Electric Company Model 25-A selenium rectifier producing 25 amps at 10 volts.

The bath, which consisted of one liter of solution, was placed in a two liter rectangular battery jar which was placed inside a three liter pyrex beaker containing water. A thermometer was suspended in both solution and water. This combination was placed upon a 750 watt Fisher Thermix magnetic stirring hotplate. A teflon coated stirring bar was used for agitation of the solution. The complete arrangement is shown in Figure 3.

Since the deposition of P is a diffusion controlled reaction, some means of agitating the solution is required, particularly at low concentrations of phosphorous acid.

Using conventional mechanical stirring and also no agitation at all it was shown that the rotating magnetic field had no apparent influence upon either the structure or the magnetic properties of the deposit.

5. Control

5.1 Bath

Bath temperature was maintained at ± 1°C by manual control of the hotplate which directly heated the water in the 3000 ml beaker. Since heat transfer from bath to water was relatively slow, only

minimal attention to the beaker temperature was necessary once the bath temperature had stabilized.

With the particular baths employed, the cathode current efficiency is low resulting in a gradual increase in the concentration of the Ni ion during plating. The deposition of P is insensitive to the Ni ion concentration over a small range but for large increases it is necessary to apply some correction. One technique is to remove a volume of the bath and replace with water, but this simultaneously reduces the phosphorous acid, phosphoric acid, and chloride as well as the excess Ni. These in turn must be replenished. During deposition the phosphorous acid is depleted by formation of the alloy. This depletion is small, but after extended use of the bath must be considered. The total result is that bath composition is a complicated problem when very precise control over the deposited alloy is desired. In this experiment, rather than perform the laborious analyses required to maintain a single bath continuously, it was decided to discard the bath after a period of use and prepare a fresh solution. X-ray fluorescent analysis was used to determine when the Ni ion had increased by a factor of 5% which was used as the criterion for discontinuance. Depletion of phosphorous acid was negligible during this period.

The bath pH, which tended to increase during deposition, was checked periodically with a Photovolt Model 125 pH meter with an accuracy of ± 0.15 pH units. The pH was maintained at 1.0 by additions of phosphoric acid.

5.2 Sample

The deposition of P is sensitive to several bath parameters. The Min-P bath was used first in which the temperature was varied in steps of 50-60-70-90°C producing w/o P values of 1.2-1.5-2.0-2.9 respectively; a linear relationship. However, it was found easier to change the composition by varying the current density as was done with the other three baths. This variation is shown in Figure 4. In order to cover the entire composition range from 0 w/o to 15 w/o P it was necessary to prepare three baths containing different concentrations of phosphorous acid. Other parameters constant, the deposition of P over the range 3 to 15 w/o is essentially a linear function of concentration of phosphorous acid.

Thickness was controlled at 10^{-3} cm (10 microns or 0.0004 inches) by regulating the time of deposition. Thickness of deposit per unit time increases non-linearly with increasing current density so the trial and error method had to be used. After removal of the substrate as described previously, thickness was determined by weighing the deposit on a Mettler B-5 analytical balance and then calculating from density and surface area considerations.

Precise knowledge of thickness was not a requisite in this investigation but a uniform sample was desired. A 2 cm square sample that is 10^{-3} cm thick is sufficiently rigid to be handled and provides a convenient weight for chemical analysis. This is also approximately the optimum thickness for x-ray transmission Laue studies.

B. Chemical Analysis

1. Equipment

Chemical analyses of the Ni-P alloys were made utilizing a Bausch and Lomb Spectronic 20 spectrophotometer.

2. Procedure

Analysis was made colorimetrically for P using the heteropoly blue method as outlined in Appendix A; Ni being obtained by difference. This procedure was used as x-ray fluorescent analysis of the alloy detected only Ni and P in quantities sufficient to have a significant effect on the result. The transmittance curve was calibrated by analyzing for Ni by standard gravimetric methods involving precipitation with dimethylglyoxime and then following with the colorimetric test for P on the same sample. It was not possible to calibrate the curve using a standard phosphate solution as there is apparently an incomplete conversion of phosphorus to phosphate when the alloy is dissolved with acid. Colorimetric analysis for P, although not as precise, is preferred over the Ni analysis since it is faster and more amenable to group runs.

C. Magnetic Measurements

The equipment is shown in Figures 5, 6, and 7 and described in Appendix B. The magnetizing field was calibrated for AC amps field current versus oersteds field strength and found to be linear from 0-700 oersteds with a value of 300 oersteds at 5 amps. The Helmholtz coil was capable of sustaining 5 amps without overheating.

A vicalloy standard, which had been calibrated using a DC loop plotter, was used to establish semi-quantitative values for saturation

magnetization. Intrinsic coercive force was measured in accordance with Appendix B.

Photographs were made of characteristic loops with the Textronic C-12 oscilloscope camera accessory. Polaroid positive/negative Type 55 P/N film was used as it provides an immediate positive plus a negative for subsequent requirements.

D. Heat Treatment

1. Equipment

Heat treatment was conducted in a Lindberg Diffusitron Mark II, M50 furnace covering 250°C to 1300°C. Basically the furnace consists of three helically wound heating coils surrounding approximately 20" of a 36" quartz tube of 2-$\frac{1}{2}$" O.D. The furnace maintains an 8" uniform hot zone at ± 0.5°C at 800°C and recovers almost instantaneously after the insertion of a sample. Once calibrated and set the instrument is extremely stable and consistent over a series of runs.

The temperature was continuously monitored with a Leeds and Northrup multiple range potentiometer indicator using a chromel-alumel thermocouple.

The furnace atmosphere was maintained as a positive flow of 10 cubic foot per hour of high purity argon gas.

2. Operation

Heat treatments were conducted for various experiments at 50°C intervals from 200°C to 800°C. As far as possible, heat treatments at a given temperature were made by combining all samples into a single batch, thus achieving the maximum uniformity of time and

temperature.

For treatment the samples were made into a sandwich consisting of alternate layers of sample and 0.025" x 0.75" x 2" aluminum oxide ceramic plate. The sandwich was wired together with nickel. This device prevented buckling of the samples during treatment as well as further improving the temperature uniformity.

E. Aging

The aging of magnetic properties was tested by allowing the samples to remain under room temperature and atmosphere for a period of four months which was the maximum time available. In addition, it was attempted to accelerate the aging in a selected group of samples by subjecting them to a temperature of 100°C for two weeks in an oven. No special atmosphere precautions were taken as the temperature was not considered high enough to cause significant oxidation. No attempt was made to relate the accelerated period to a normal time period and consequently a positive aging effect would probably be of most significance.

F. X-Ray

1. Equipment

A General Electric XRD 5 x-ray unit was used with a No. 2 SPG detector and the necessary accessories for diffraction and fluorescence. The conventional tungsten target tube was used for fluorescence with a lithium fluoride analyzing crystal and a copper target tube was used for all diffraction. Photographs were made with a G.E. XRD powder camera having a 114.6 mm radius, G.E. XRD Laue camera, and a Polaroid XR-7 Land Diffraction Cassette. The cassette was used with

polaroid film in place of the XRD Laue camera in transmission studies when conducting preliminary investigations where speed was a requirement and no negative was desired.

2. Fluorescent Analysis

The following items were chemically analyzed for impurities with the indicated results at tube settings of 50 kv and 20 ma:

Nickel Anode

Trace Co
Fe
Mn

Copper Foil

No impurities detected

Copper Coupon

Trace Fe

Nickel-Phosphorus Alloys of Various Compositions

Trace Co
Fe
Mn
Cu

Plating Baths

Trace Cu

These impurities would be expected in each case.

3. Structure Analysis

3.1 Debye-Scherrer

It was found convenient to deposit the Ni-P alloy onto a 0.010" soft copper wire which was then used as the sample in the powder camera. Control of composition is more difficult

in this technique because of the shape and small surface area of the substrate but can be held within reasonable limits using the data of Figure 4 and careful attention to the current density. The copper pattern can be suppressed by depositing a thick layer of alloy but if allowed to appear serves as an excellent standard for calibrating the film. The copper pattern is easily recognized since it has a much larger grain size than the alloy and appears as spotty lines as opposed to the solid lines of the latter.

The tube parameters were 45 kv and 17 ma with a nickel filter foil used to eliminate the unwanted K-beta radiation. Exposure time was generally ten hours for Kodak SP 351 x-ray film.

3.2 Transmission Laue

Transmission was chosen over back reflection because of the intense scattering in the latter which tends to obscure the pattern in the high angle region. In addition there are a very large number of lines which are close together in the back reflection region and are therefore difficult to index properly.

Parameters for the copper tube were again 45 kv and 17 ma. With 10 micron thick material exposure was generally 3 hours for Polaroid 3000 speed Type 57 film at 3.2 cm specimen to film distance and 5 hours for standard Kodak Medical x-ray film at 3.82 cm specimen to film distance.

All Laue photographs appearing in the Figures section were made on Kodak film at 3.82 cm specimen to film distance.

3.3 Orientation

Electrodeposited films characteristically have a preferred

orientation created by the tendency of the grain to grow vertically faster than horizontally. This produces a fiber texture whose axis is perpendicular to the plane of the deposit. If the film is placed in the conventional sample holder for Laue transmission, the fiber axis is parallel to the x-ray beam and any orientation present will not be detected since only continuous Debye rings will be produced.

To overcome this, a sample holder was constructed of a hollow plastic tube which had one end cut off at an angle of 45° to the tube axis. The sample was taped to this end and hence was at an angle of 45° to the x-ray beam.

The holder was used with the transmission Laue accessories and photographs were made as before.

G. Metallographic

Samples which had been plated on the copper coupons were mounted in Epocast epoxy resin for metallographic tests. As an electrolytic etch was dictated, a fine copper wire was attached to the samples away from the area to be exposed. The wire protruded from the top of the mount and served as a lead wire to the (+) battery terminal making the sample the anode as required in electrolytic etching. The etchant was placed in a stainless steel pan which was connected to the (-) battery terminal and served as the cathode.

Some samples were mounted in the standard upright position exposing the side view of the deposit. Other samples were mounted almost horizontally by placing one end on a small piece of 0.060" thick metal. Essentially a top view is then presented. This technique is used generally to obtain a geometrical advantage when

measuring thickness of extremely thin deposits. Here it afforded a different perspective of the material.

The mounts were given a rough wet grinding by hand on a Buehler Handimet 1470 AB Grinder with grit sizes in order 240, 360, 400, and 600. The intermediate polish was on a rotating cloth wheel with 6 micron diamond paste followed by 1/4 micron. Final polishing was done on a Syntron, an automatic vibratory device, using slurries of Linde A and Linde B in that order.

Ni-P, like pure Ni, is difficult to etch. The following solution was developed and used at 1.5 volts:

HCl	-	100 ml
H_2O	-	100 ml
HNO_3	-	5 ml
$FeCl_3$	-	saturated

The straight HCl-$FeCl_3$ etchant was found to stain excessively. Time of etch, usually 30-60 seconds, was regulated to give the desired contrast. There appeared to be a direct correlation between the w/o P and resistance to the etchant.

Polished and etched samples were examined using a Reichert Zetopan M binocular microscope which was equipped with a Polaroid camera. Appropriate photographs were made with Polaroid P/N film.

III. RESULTS

A. Structure

1. X-Ray

Deybe-Scherrer photographs were made of a series of plated wires covering the range 0-15 w/o P both in the as-plated condition and after annealing for four hours at 400°C under an atmosphere of argon.

Wires of as-plated low w/o P showed only a pure Ni pattern. There was no apparent shift in the d-spacing, which could be an indication of very little solid solubility of P in the Ni terminal solution but that conclusion cannot be drawn because the effect on the lattice of Ni by the solution of P is not known. At higher P values some wires yielded no pattern at all while others showed a single, so-called amorphous halo at the d-spacing corresponding to the Ni (111) reflection. This halo, as mentioned in the Introduction, has been taken as proof that the deposit has assumed an amorphous structure with no evidence of crystallinity. The transition point appeared to be 5 w/o P.

After heat treatment, three characteristic patterns as seen in Figures 8, 9 and 10 were observed. Figure 8, characteristic of less than 8 w/o P showed the pure Ni pattern superimposed upon another pattern of extreme complexity. This latter pattern's intensity was seen to vary directly in proportion to the amount of P present; the Ni intensity varying inversely. The d-spacings and relative intensities for the complex pattern are shown in Table 2. For alloys of approximately 8-14 w/o P, only the complex pattern, which is shown in

Figure 9, was evident.

Consider the Ni-P phase diagram in Figure 1. Figure 9 should represent the Ni_3P precipitate whose concentration will be directly proportional to the w/o P in the alloy. Unfortunately the d-spacings for Ni_3P are not to be found in the literature or the ASTM card file. Nowotny[17], who is usually referenced on this subject, identified the unit cell of Ni_3P as tetragonal with extinction for planes where $h + k + l \neq 2n$ and gave the lattice parameters as $a = 8.916$ Å, $c = 4.389$ Å. The d-spacings can be calculated from these values using the relation

$$\frac{1}{d^2} = \frac{h^2 + k^2}{a^2} + \frac{l^2}{c^2}$$

This was done and is shown in Table 2. It is seen that there is quite good agreement between the two so that Figure 9 must in fact be Ni_3P.

Figure 10 was characteristic of most greater than 14 w/o P samples. Despite its strong similarity to Ni_3P, it is seen to be a distinctly different pattern. The limited number of d-spacings is a result of a poorer exposure of the film. There was no evidence of the two patterns coexisting although this fact might be obscured by the similarity between the two. Figure 10 cannot be explained from the phase diagram. Upon passing 15 w/o P a two phase region is entered and two patterns should be superimposed with Ni_3P dominating on the low P side. The alloys in question all fall in this category. It was assumed at this point that Figure 10 was a metastable phase which tended to disassociate into Ni_3P. Other high-P wires were heat treated at 700°C for 1 hour to investigate this conjecture.

TABLE 2

Lattice Spacing and Relative Intensity

Figure 10		Ni_3P		Figure 11	
d, Å	I	d, Å	hkl	d, Å	I
2.92	W	2.95	211	2.97	W
2.88	VW	2.82	310		
2.46	M	2.46	301	2.38	M
2.23	VW	2.23	400		
		2.19	002	2.20	M
2.15	VS	2.15	312	2.15	S
2.10	M	2.10	330	2.10	VW
2.06	M	2.07	112		
2.03	M	(Nickel)			
1.998	M	1.993	420	1.994	VW
1.967	W	1.968	202	1.957	W
1.939	VS	1.939	411	1.910	VS
				1.877	S
				1.838	W
1.800	M	1.801	222		
1.756	M	1.748	510		
1.732	S	1.731	312		
1.657	M	1.652	501	1.672	M
1.583	VW	1.576	440	1.580	VW
1.566	W	1.563	402		
1.552	VW	1.549	512	1.549	W
1.536	W	1.529	530		
1.522	VW	1.517	332		
1.478	VW	1.475	422	1.497	M
1.441	VW	1.443	103		
1.413	M	1.409	620		
1.395	M	1.390	611		
1.371	W	1.373	213		
		1.367	512		
1.334	W	1.327	541	1.344	M
1.315	W	1.312	303		
1.280	W	1.280	442		
		1.272	631		
1.260	S	1.260	550	1.253	M
		1.259	323		
1.245	W	1.254	532		
		1.236	640	1.234	S
1.229	W	1.230	602		
		1.223	701		
1.215	M	1.211	413		
1.189	S	1.186	622		

TABLE 2 (cont'd)

Figure 10		Ni_3P		Figure 11	
d, Å	I	d, Å	hkl	d, Å	I
		1.179	721		
		1.170	730		
1.135	M	1.131	433		
		1.114	800		
1.107	M	1.104	651		
1.099	S	1.097	004		
		1.096	523		
1.091	W	1.093	552		
1.082	S	1.081	820		
		1.080	114		
1.065	M	1.065	204		
1.045	W	1.050	660		
1.038	M	1.036	224		
		1.035	613		
		1.032	732		
1.022	S	1.022	314		
1.017	W	1.015	831		
		1.008	543		

NOTE: Does not include values above 3.00 and below 1.00. In hkl; h and k may be interchanged.

TABLE 3

Lattice Spacings for Hexagonal Nickel

d, Å	hkl
3.741	001
2.294	100
1.956	101
1.870	002
1.449	102
1.324	110
1.248	111
1.247	003
1.147	200
1.097	201
1.095	103
1.081	112

NOTE: Does not include values above 4.00 and below 1.00. In hkl; h and k may be interchanged.

Only the Ni_3P pattern was observed.

Attention was given to other possible compounds which might have produced these patterns such as copper and nickel oxide, other phosphides of nickel (Ni_2P, NiP_2, Ni_7P_3), phosphorus, phosphorus oxide and nitride, and phosphorous acid. None were indicated.

Hexagonal nickel was also considered since it has been variously reported in the literature. Pearson[18] gives the lattice spacings for a hexagonal nonmagnetic form of Ni as, a = 2.65 Å, c = 4.32 Å from which the d-spacings shown in Table 3 were calculated from the relation

$$\frac{1}{d^2} = \frac{4}{3a^2}(h^2 + hk + k^2) + \frac{4}{3c^2}(l^2)$$

Hexagonal nickel does not appear to be involved. Pearson, in the previous reference, stated that its existence is generally disputed and where reported it may have actually been some nickel hydride, nitride, carbonyl, etc.

Lattice spacings below 1.00 Å were not determined because the Debye-Scherrer films were too diffuse in the high angle region. Also there are so many closely spaced lines to be found that identification is impossible without the relative intensity data which is usually afforded by the ASTM file.

Most of the x-ray analysis was based on the transmission Laue studies. The Laue photographs were quicker and easier to obtain and the actual magnetic test sample could be used as the specimen rather than the contrived specimen of the plated wire used in the Debye-Scherrer technique. This latter method, however, was in-

valuable in that it yielded accurate lattice spacings which were then used to index and identify the Laue photographs. With the Laue method it was possible to investigate a more accurate composition range and to consider the effect of heat treatment in a more detailed manner.

Figure 11 shows the characteristic halo of as-plated, medium to high phosphorus alloys. The halo is shown in Figure 12 compared to the Debye rings of pure Ni. It can be seen that the halo spreads out on either side of the (111) reflection. Goldenstein[19] noted a possible shift of the halo to the outer side of the (111) ring and related this to similar effects with known amorphous materials. This halo has been the basis for the amorphous structure which has been ascribed to electrodeposited Ni-P and to the electroless variety as well by other investigators.

However, it is the belief of the author that both systems are not amorphous but rather supersaturated solid solutions of P in crystalline Ni of very fine grain size which decreases in direct relation to the w/o P of the alloy. Graham[20], using electron diffraction, has estimated the grain diameters to be less than 100 $\mathring{A}$ in electroless Ni-P which shows analogous x-ray behavior to the electrodeposited system.

From the Scherrer formula for particle-size broadening

$$B = \frac{k\lambda}{s \cos\theta}$$

where k and λ are constants and s is the average particle size, it may be seen that two variables contribute to broadening; s and cos θ. Cos θ will not be considered since its values for the (111) and (200) reflections are 0.925 and 0.898 respectively; a difference insufficient to affect the problem being considered. Given equal intensities for all lines we could consider the effect of cos θ, but this is not the case particularly in the transmission region of Ni where the (111) is several times more intense than the (200). Therefore the particle size is the dominant factor.

If the particle size becomes small enough then broadening may occur to the extent that a given line will vanish from the pattern. A good estimate of s for which the pattern fades altogether is 100 $\mathring{A}$. It will be noted that this is also the grain diameter given previously by Graham for the electroless system. The value cannot be determined exactly because the Scherrer formula fails quantitatively at these values of s because of the mechanical difficulty of measuring B.

Figure 13 is a pattern of a 2.9 w/o P as-plated alloy in which the outer ring which is the (200) reflection has become diffuse while the inner ring which is the (111) reflection remains strong although showing some broadening. After heat treatment at 400°C for 3 hours the intensity of the (200) reflection became relatively stronger equivalent to that for pure Ni in Figure 12. A 4.9 w/o P alloy, intermediate in composition to the materials of Figures 11 and 13, had a single, slightly diffuse (111) ring which had not broadened to the extent of the halo. The (200) reflection was completely ab-

sent. The (111) reflection resists fading because of the intensity factor, thus the halo and all the above effects can easily be explained from particle size broadening.

A further argument to substantiate a small crystalline structure for this system, based on magnetic effects, is presented in a later section.

Heat treatment of alloys having a halo pattern as-plated, results in a very rapid conversion to crystallinity detectable by Laue transmission. 5 minutes at 400°C for a 9.6 w/o P alloy yielded the pattern of Figure 14. This is a superimposed pattern of Ni - Ni_3P. It would seem, as has been argued by others, that this speed of reaction attests to the prior existence of crystals in the as-plated structure. This alone, however, is not proof of that fact.

Figure 15 shows a comparison between a 7.6 w/o P alloy and a 11.3 w/o P alloy both of which were heat treated at 400°C for 3 hours. We see a strong Ni and a weak Ni_3P pattern in the former and just the opposite in the latter. Assuming complete precipitation of all P as Ni_3P, the two alloys are 50% nickel and 25% nickel respectively. Thus the transmission Laue as well as the Debye-Scherrer data corroborates the predictions of the phase diagram in terms of the Ni-Ni_3P two phase reaction.

The Ni (111) reflection, when weak, can be obscured by the several reflections for Ni_3P in its vicinity and a medium intensity Ni_3P reflection is found in the same position as the Ni (200). There is also a limit of detection in the method which prevents the identifi-

cation of small amounts of Ni or Ni_3P in the matrix of the other. The result is that it is difficult by Laue methods to describe the presence of small concentrations of Ni in Ni_3P and vice versa.

A tendency for grain growth in the Ni_3P precipitate was detected and found to be directly proportional to the amount of P present. The Ni was not so affected to the same degree. Figure 16 of a 11.0 w/o P alloy at 400°C for 3 hours shows smeared rings indicative of growth while identical conditions for a 14.0 w/o P alloy produced the spotty rings of Figure 17 which result from even more growth. In Figure 16 the solid rings of Ni can be clearly seen showing that growth is at least restricted. Ni rings are not seen in Figure 17 because the matrix is essentially all Ni_3P. The alloy of maximum P tested, 15.7 w/o, having received the same treatment as the others produced a Laue pattern of spots with no evidence of rings. This is characteristic of very large grains. Thus the effect of heat treatment on the microstructure through coalescence and grain growth of the Ni_3P will proceed at a rate dependent upon the composition. This will subsequently be shown to have an effect on the magnetic properties.

The NiP(x) pattern mentioned in the preceding Debye-Scherrer section was again found in high-P alloys and as before appeared to be metastable. Spotty rings of Ni_3P can be seen in Figure 18 superimposed upon the continuous rings of NiP(x). This represents a transition structure. For low temperature-short duration (400°C-15 min.) heat treatment, only NiP(x) was found. At higher temperatures and/or longer times, NiP(x) decomposed eventually leaving only Ni_3P.

Orientation was detected in the heat treated alloys as seen in Figure 19. However, only the Ni proved to be involved having a fiber texture calculated from the photograph as a strong (111) oriented normal to the plane of the film. Note the ring with intense arcs. This is the Ni (111). The (200) arcs are not evident in this photograph but were found in others. This is a further indication of as-plated crystallinity. Electrodeposited Ni has been variously reported as having (100) or (112) and (113) or (110) or (111) textures depending upon the baths and plating parameters employed. It seems incongruous to explain the (111) orientation on the basis of the material having assumed that structure from the amorphous state without the Ni_3P also showing a similar effect. No texture was found for this compound in any sample regardless of composition or metallurgical history. Graham[21] found a preferred orientation in the initial particles of Ni_3P precipitated from electrolessly deposited Ni studied over the range 4.5 to 9.5 w/o P. The only explanation that can be offered is that the orientation of the Ni induces orientation in the Ni_3P which forms immediately in contact with it, but that the influence is short lived.

An attempt was made to show the effect of changing the heat treatment parameters upon the orientation by annealing over a series of temperatures and/or time intervals. No effect was found. The extent and degree of the orientation did not change within the limits of detection of the method.

2. Metallographic

A peculiar, heretofore unexplained, microstructure has been identified in electrolessly plated metals such as copper and nickel and has been reported for electrodeposited Ni-P[22]. Found in this investigation and shown in Figure 20, it is characterized by lamellae running parallel to the substrate. One theory explains the bands as due to composition variation which in this case means that there is a sinusoidal gradient of the P concentration through the plate. Upon heat treatment, this causes a preferential precipitation of Ni_3P at the points of maximum P content leading to the dark bands of the etched sample. That this is the case is seen more clearly in Figure 21 where the precipitate has coalesced under the influence of the higher annealing temperature with the lamellae yet remaining distinct.

The precipitate is seen in another perspective in Figure 22 and Figure 23, both of which are top views. The latter represents the coalescence of the fine precipitate of the former under the influence of a higher annealing temperature. Figure 22 has a grayish appearance due to the dispersion of the Ni_3P.

Figure 24 is a top view which shows the Ni_3P to exist in sheets. Note the circular shapes. In this perspective the lamellae have been shaved off at a very small angle exposing alternate layers of Ni-rich material and the dark Ni_3P-rich material. It must be remembered that the lamellae are not flat but rather wavy in three dimensions which accounts for the peculiar circular shapes.

High-P alloys above about 12 w/o were found to be free of the lamellar structure and tended to form large, easily distinguishable grains of Ni_3P and/or NiP(x) as seen in Figure 25. Ni_3P was not found in the same metallographic form as before where it appeared as a precipitate.

A study was made of the relationship of the lamellar structure to the composition of the alloys. Over the range 6-12 w/o P the lamellae appeared independent of composition and were spaced at approximately 1.5 microns (1.5×10^4 Å). The bands were relatively wide so that the light area between was generally much smaller and ranged from 0.1 to 1.0 microns in width. A 4.4 w/o P alloy was found to have a very slight indication of lamellae at the plate edge but none elsewhere. None of the alloys of less P had the lamellar structure which must then develop over the range 4-6 w/o P. From 12 to 14 w/o the lamellae were found to be very indistinct. They were completely absent above 14 w/o.

The as-plated alloys tended to become brittle with increasing P. This factor was intensified by heat treatment with the high-P alloys becoming extremely brittle. Brittleness is a well known attribute in Ni-P and it has been observed that prolonged heat treatment produces a significant recovery of strength in low-P alloys but much less in high-P alloys. In the metallographic study many cases were found in which heat treated films had cracked because of differences of thermal expansion between the deposit and the copper substrate. All cracks proceeded along the lamellae or at right

angles between them. As a hypothesis for the embrittlement it is proposed that the Ni_3P is structurally weak and when existing in sheets, as in the lamellae, forms a natural cleavage system. Upon coalescence with heat treatment the lamellae are destroyed and the film strength increases because the cleavage network has been reduced. High-P alloys do not recover their strength because the weak Ni_3P constitutes a major portion of the film volume.

B. As-Plated Magnetic Characteristics

As-plated pure Ni and alloys out to about 2 w/o P were found to have considerable variation in the Hci (intrinsic coercive force). For pure Ni the values ranged from 105 Oe (oersteds) down to 25 Oe, but generally were about 75 Oe as is the case in the hysteresis loop of Figure 26. Stress was thought to be responsible and was demonstrated to be the causative agent by stress-relief annealing the samples at 200°C for 4 hours. The Hci was reduced in most samples to a uniform value of about 25 Oe. There was a similar effect with Mr (remanent magnetization) which is structure sensitive as is Hci. Ms (saturation magnetization), being structure insensitive, was found to change but little.

Data for alloys out to 2 w/o P was limited due to the small number of samples produced in this range. The data that was obtained was inconclusive because of scatter, the error probably being compounded by stress and other unidentified factors. With increasing P both the Hci and Ms decreased with the loops becoming smaller and

smaller. A typical restricted loop is shown in Figure 27 taken at an instrument setting 10X in the vertical of Figure 26. At the same sensitivity as before the latter hysteresis loop would be barely visible. Beyond 6 w/o P the sensitivity of the instrument was passed and the loops disappeared altogether.

The behavior of the Ms and the Hci with composition is shown in Figure 28 and Figure 29 respectively. Figure 28 represents as-plated alloys but in Figure 29 the alloys were stress-relief annealed at 200°C for four hours in an attempt to eliminate the effect of stress. Alloys above 2 w/o P were unaffected by the anneal. 200°C has been shown to have no detectable effect upon the microstructure. It appears from these observations that there is a maximum in the Hci at approximately 4 w/o P.

Testing with a strong magnet showed that the magnetic character persisted up to 8.0 w/o P beyond which all alloys were nonmagnetic. As discussed in the Introduction, Kotel'nikov[23] attributed this attenuation to the development of an amorphous structure. That this is not the case in the electrodeposited system is demonstrated by the fact that the amorphous halo in x-ray patterns appears in alloys which have at least a minimum of 4.9 w/o P, but clearly show ferromagnetic behavior. The attenuation is actually the result of the combined effect of two magnetic phenomena.

Alloying a nonmagnetic material such as P with a ferromagnetic material such as Ni results in a suppression of the net magneti-

zation and also the coercive force which is, in a sense, a function of the magnetization. Both of these effects were found as shown in Figures 28 and 29. This behavior can be explained with band theory as covered in Bozorth's and Wert's books listed in Section VI. The nonmagnetic material contributes electrons to the ferromagnetic material's unbalanced half band in such a way as to reduce the magnetization. At a sufficient composition the half bands are completely balanced and the alloy is nonmagnetic, as for instance a 32-68 Cu-Ni alloy at room temperature.

The effect of alloying P in Ni is not known but by analogy to antimony it could be concluded that 8 w/o P is sufficient to account for the attenuation by the alloying effect. However the solid solubility of P in Ni is reportedly extremely low; quite the opposite for Sb in Ni. Also we have evidence that the supersaturated P is highly segregated as for instance in the lamellae. Therefore it is proposed that the effective alloying composition of P in Ni is insufficient to account for the attenuation and we must look to another phenomenon to complete the explanation.

It has previously been proposed that the material has an extremely fine grain structure. It is further proposed that the grains are so small that the material is subject to a fine particle effect.

Fine particles of ferromagnetic materials have been shown theoretically and experimentally to have the character indicated in Figure 30. This is a schematic for purposes of discussion and is

not to be construed as numerically representing the Ni of this investigation. With decreasing particle size, the magnetic domains become single and the coercive force rises because a change of magnetization can occur only through rotation of the magnetization vector which requires more energy than a domain wall movement that would occur were the material multi-domained. The critical radius for a spherical particle of Ni below which only single domains exist has been calculated to be 520 Å[24]. Graham[25] has estimated the grain diameter to be 100 Å in electroless Ni-P which has an identical attenuation. From the x-ray line broadening, an estimate of 100 Å can be made for the particle size in the electrodeposited system.

Neel[26] has theoretically proposed that when particles become quite small the coercive force falls because thermal vibrations prevent them from sustaining a stable magnetization. There is another critical size below which the disordering effect of the thermal vibrations completely overcomes the magnetization vector and ferromagnetic behavior ceases to exist at temperatures above absolute zero. In Figure 30 this is seen as a decrease toward zero Hci with decreasing particle size.

To test the applicability of these two theories in the electrodeposited Ni-P system a simple experiment was devised. From the last considered theory it follows that lowering the temperature should diminish the thermal disordering and push the critical value to smaller particle sizes so that nonmagnetic alloys could be shown

to be magnetic below some temperature. But at the same time it must be understood that the decrease in magnetization with alloying in the first theory is also representable as a linear decrease in the Curie point so that with P in Ni the Curie point would be room temperature at 8 w/o P. Lowering the temperature here brings the alloy below its Curie point and restores its magnetic character. Hence it is difficult to separate the applicability of the two theories by temperature effect alone.

The films were suspended in liquid nitrogen at -196°C to temperature equilibrium and then quickly placed in the loop tracer. The films heated rapidly but the predicted effect was easily seen. The hysteresis loops appeared for alloys completely nonmagnetic at room temperature, even to the limit of sensitivity of the instrument at approximately 14 w/o P. From pure Ni to less than 4 w/o P there was no observable effect probably, for the alloys, because of being obscured by the rapid heating. But for 6 w/o P there was a dramatic change with the loops approximating those of annealed pure Ni. From this point the loops were seen to become smaller and smaller out to the limit of instrument sensitivity. This is a demonstration of the lower temperature having pushed the critical particle size to smaller values and/or having brought the alloys well below the room temperature Curie point. As a given film warmed to room temperature the hysteresis loop could be observed to dynamically extinguish itself.

Undoubtedly both theories are at work in the as-plated system. In Figure 29 we have an indication of a maximum Hci as predicted by Figure 30. Consider that the alloying suppression reduces the coercive force below what it might otherwise be. This indicates fine particle behavior but is somewhat inconclusive because of the unknown contribution due to stress which is unrelievable by annealing. Thus the ferromagnetic attenuation at 8 w/o P is a result of the combined effects of alloying and fine particle with the latter dominating at small particle sizes.

The tail on the curve in Figure 29 running from 6 to 8 w/o P probably results from nonuniform particle size. At 6 w/o most particles are below the critical size for magnetism. Some inordinately large crystals are present, however, and account for the continuance of ferromagnetism out to 8 w/o where the sensitivity of the strong magnet is exceeded. Actually, it is not unreasonable to suspect that even at this composition there is a weak ferromagnetism because of this particle size effect.

The restoration of magnetic character below room temperature is an indication in itself that the attenuation is not due to an amorphous structure as discussed in the last section. Were the structure amorphous then it would not be expected to have ferromagnetic properties.

C. Heat Treated Magnetic Characteristics

Magnetic properties were found to be dependent upon time and temperature of heat treatment as well as upon composition. The

variation of Hci with composition is shown in Figure 31 with a time and temperature selected to achieve the maximum magnetic character obtained in the investigation. For a given alloy selected from the range producing maximum magnetic character, the variation of Hci with temperature at a given time is shown in Figure 32. For the same alloy, the variation of Hci with time at given temperatures is shown in Figure 33. These graphs serve only to generalize the behavior and are not all-inclusive because of the complicated inter-relationship of the factors of composition, time, and temperature.

This behavior can be explained by treating the material as a fine particle aggregate as was done for the as-plated alloys in the previous section. There are, of course, certain important differences which will be discussed. If this be the case, then what we are observing in these graphs is just a manifestation of the behavior predicted by Figure 30.

We know from metallographic and x-ray analysis plus consideration of the Ni-P phase diagram that alloys of greater than 14 w/o P have little or no free Ni and exist as large grains of Ni_3P and/or NiP(x) without the laminated structure. Figure 31 shows that these alloys are also nonmagnetic. Films having x-ray patterns showing them to be entirely Ni_3P or entirely NiP(x) or a mixture were found to be completely nonmagnetic with the exception of a few which had a very slight indication of a hysteresis loop explainable as being

due to a minute amount of Ni being present in the nonmagnetic matrix. Lowering the temperature of Ni_3P films failed to produce any evidence of magnetic character. From this, it is apparent that the magnetic characteristics of all the alloys proceed directly from the Ni and the Ni_3P is involved only indirectly through its influence upon the structure of the deposit.

It is also possible that Ni could be present in the Ni_3P - NiP(x) matrix but be so dispersed that particle size would be below the critical value so that alloys of less than 100% Ni_3P could still be nonmagnetic. There is some indication of this since the phase diagram predicts that 15 w/o P is the transition point.

Remembering the metallographic analysis on the laminated structure we see that there is a direct correlation between it and the flat portion of Figure 31 which shows the maximum Hci obtained being independent of composition over the range of 6-12 w/o P. This was also the range over which the lamellae, which have been described as sheets of precipitated Ni_3P, were present. It is then proposed that these lamellae restrict the growth of the Ni particles under the influence of heat treatment. Figures 32 and 33 are indicative of this growth factor. Higher temperatures and/or longer periods of heat treatment serve to destroy the lamellar structure through coalescence of the Ni_3P precipitate as was shown in Figures 23 and 25. Thus Ni particle growth may proceed at a more rapid rate than in the case where the lamellae are intact. This particle growth

continues until a constant coercivity of about 25 Oe is reached, and this may be noted as being the value for annealed pure Ni as observed in this investigation.

The lamellae are apparently independent of composition in terms of size and spacing and therefore constrain the Ni to an equal particle size over the entire range of 6-12 w/o P. An apparent independence of Hci with composition over this range results. The quantity of Ni particles, however, is dependent on the composition as more P means more Ni_3P and hence less Ni. Figure 34 is a hysteresis loop of an alloy from the low end of the range while Figure 35 is a loop of an alloy from the high end of the range. Both have approximately equal Hci. From cross-sectional area considerations alone the saturation magnetization value of the 7.6 w/o P alloy should be 0.30 of that for the 11.3 w/o P alloy but is only 0.10 instead. Based on 15 w/o P representing 100% Ni_3P and 0% Ni, the 7.6 w/o P alloy is approximately 50% Ni and 11.3 w/o P alloy is approximately 25% Ni. Multiplying this factor of 0.50 with the area factor of 0.30 we have 0.15, which is in reasonable agreement with that observed, considering the approximations required. This linearity of saturation magnetization with composition was found completely across the range in question.

Because the lamellae are absent below 6 w/o P the particles are unrestricted in growth and virtually precipitate into crystals beyond the limit of maximum coercivity.

Temperatures below 400°C were not exhaustively analyzed for it was apparent that any attempt to that end would be of little value. Three hours at 250, 300, and 350°C produced but minimal ferromagnetism in as-plated nonmagnetic alloys. The same time at 200°C produced no change. Goldenstein[27] has shown that 21 hours at 200°C produces no detectable change in the as-plated structure of electroless nickel.

An attempt was made to reverse the effect of coercivity degradation at high temperatures by reheat treating at 400°C some representative alloys which had originally received 2 hours at 700°C. These were magnetically tested after intervals of 1, 3-½, and 6-½ hours but no effect was noted, hence the degradation was concluded to be irreversible as it would be if resulting from particle growth.

Further, the effect of the air quench given the alloys was studied by permitting some to furnace cool under argon after 1 hour at 400°C. The Diffusitron furnace cools very slowly requiring more than 12 hours to reach room temperature from 400°C. The coercivity degraded to a value equivalent to samples which had received a 400°C treatment for 6 hours and then been air quenched. Apparently the air quench serves only to arrest the particle development.

The factors of shape anisotropy and orientation texture cannot be entirely discounted but were mostly discredited as playing any major role. In a previous section the material was shown to have a

(111) orientation normal to the film. This is also the easy direction of magnetization for Ni. Therefore, should the Ni be present as cylindrical rods whose axes were normal to the film, a large coercive force could be expected because of the combined influence of the factors. The magnetization vector would be required to move out of the easy direction into a harder direction which was also less favorable dimensionally, being several orders smaller than the former. However, examination of the Debye-Scherrer photographs for evidence of selective line broadening, which is found in cases of shape anisotropy, was negative on that count. Since there are only 8 lines available for Ni and the pattern is somewhat obscured by Ni_3P, a clear-cut evaluation of this point could not be made. Also, it would be expected that the Ni would not take this shape because of the lamellae. Any shape anisotropy should be in a direction parallel to the film.

One further point needs to be discussed. In the last section we saw that there was an apparent maximum in the Hci of about 80 Oe due to particle size effects, yet in this section a maximum of 180 Oe was found. In the as-plated condition the material exists as particles which are alloys of Ni with substantial percentages of P. The P restricts the magnetic character of the Ni through the effect of alloying. With heat treatment Ni precipitates and grows by rejecting P or Ni_3P into a nonmagnetic shell around the developing nucleus. The magnetic Ni is the terminal solution

of the Ni-P phase diagram containing very little P and therefore does not suffer the inhibiting influence of the alloying. The nonmagnetic shell further enhances the behavior of the Ni as a "free" particle permitting more adherance to fine particle theory.

D. Aging

There was no aging detected under either the four months standard conditions period or the two weeks at 100°C accelerated period. If the basis for coercivity is as we have outlined then none should be expected because particle growth could not occur to any measurable degree without a temperature at least in excess of 200°C.

The findings of Koretsky[4] mentioned in the Introduction cannot be explained. His aged coercivity of 180 Oe approximates the maximum obtained in this investigation. Nothing was achieved to parallel the 250 plus Oe which he reported. Since no background information was given as to the method of preparation, etc., it can only be conjectured that the difference between 250 and 180 Oe was due to some other factor such as stress, which was relievable with time.

CONCLUSIONS

The principal findings of this investigation of the magnetic properties of the electrodeposited nickel-phosphorus system are as follows:

The maximum w/o P which can be obtained in an acceptable alloy film is approximately 15, which corresponds to 100% Ni_3P when precipitated.

The as-plated alloy exists as a supersaturated solid solution of P in crystalline Ni at all compositions. Any other constituents which might have been present were in quantities too small to be detected by the x-ray methods used.

With increasing P the grain size decreases. At approximately 5 w/o P the grain size is such that x-ray transmission Laue photographs show only the so-called "amorphous halo". The halo, however, is not due to an amorphous structure but rather the small grain size. The amorphous structure which has been assigned to this system results from its "anomalous" x-ray behavior.

Magnetic characteristics of as-plated alloys can be explained on the basis of the effect of alloying and by adapting fine particle theory. Both factors are involved with the latter dominating in the vicinity of the magnetic-attenuation composition of 8 w/o P. Here the grain size and hence the magnetic domains reach a critical size at which the thermal vibrations prevent the formation of domains and reduce the net magnetization to zero. Lowering the temperature

restricts the thermal vibrations and pushes the critical size to smaller values so that alloys of greater than 8 w/o P can be shown to be magnetic. The effect can also be construed as lowering the temperature of the alloys to a point below the room temperature Curie point.

Magnetic characteristics of heat treated alloys can be explained by fine particle theory alone as the effect of alloying is virtually eliminated with the precipitation of Ni_3P.

In heat treated alloys only Ni, Ni_3P, and NiP(x) were detected. The latter is a metastable phosphide which decomposes with time and temperature forming Ni_3P. The Ni is the Ni terminal solution of the Ni-P phase diagram containing an undetermined but small amount of P.

Ni_3P and NiP(x) are completely nonmagnetic at room temperature as are heat treated alloys of greater than approximately 14 w/o P which contain only these compounds. The Curie point for both appears to be below the boiling point of liquid nitrogen (-196°C).

All magnetic properties derive directly from the Ni. P has an indirect influence through alloying, structure effects, and the formation of the nonmagnetic compounds.

Over the range 6-12 w/o P the film structure upon heat treatment is lamellar. The lamellae, resulting from a sinusoidal P composition gradient, are parallel to the substrate and consist of alternate sheets of Ni_3P-rich and Ni-rich material. Above 12 and below 6 w/o P the lamellae are degenerate or absent.

Maximum attainable coercivity is associated with the lamellar structure presumably because of its influence on particle size.

The dimensional structure of the lamellae is independent of composition and hence induces the Ni particles into a constant size with given conditions over the entire range. Therefore the coercivity is independent of composition over this range.

The Ms and Mr are linearly dependent on the composition over the range, depending on the amount of Ni present.

Below 6 w/o P the absence of lamellae permits the Ni to coalesce too rapidly to achieve maximum coercivity.

With increasing time and temperature of heat treatment the coercivity degrades, eventually reaching a constant value of approximately 25 Oe, which is also the value for annealed pure Ni found in this investigation.

Aging does not occur because particle growth is absent unless heat treatment is applied.

Inasmuch as the as-plated structure of the electroless Ni-P system is analogous to the electrodeposited system, the magnetic characteristics of both should also be analogous.

Brittleness of the films is a function of the lamellae which act as cleavage planes. Destruction of the lamellae through coalescence from heat treatment reduces brittleness in low-P alloys but not in high-P alloys because the matrix remains largely Ni_3P.

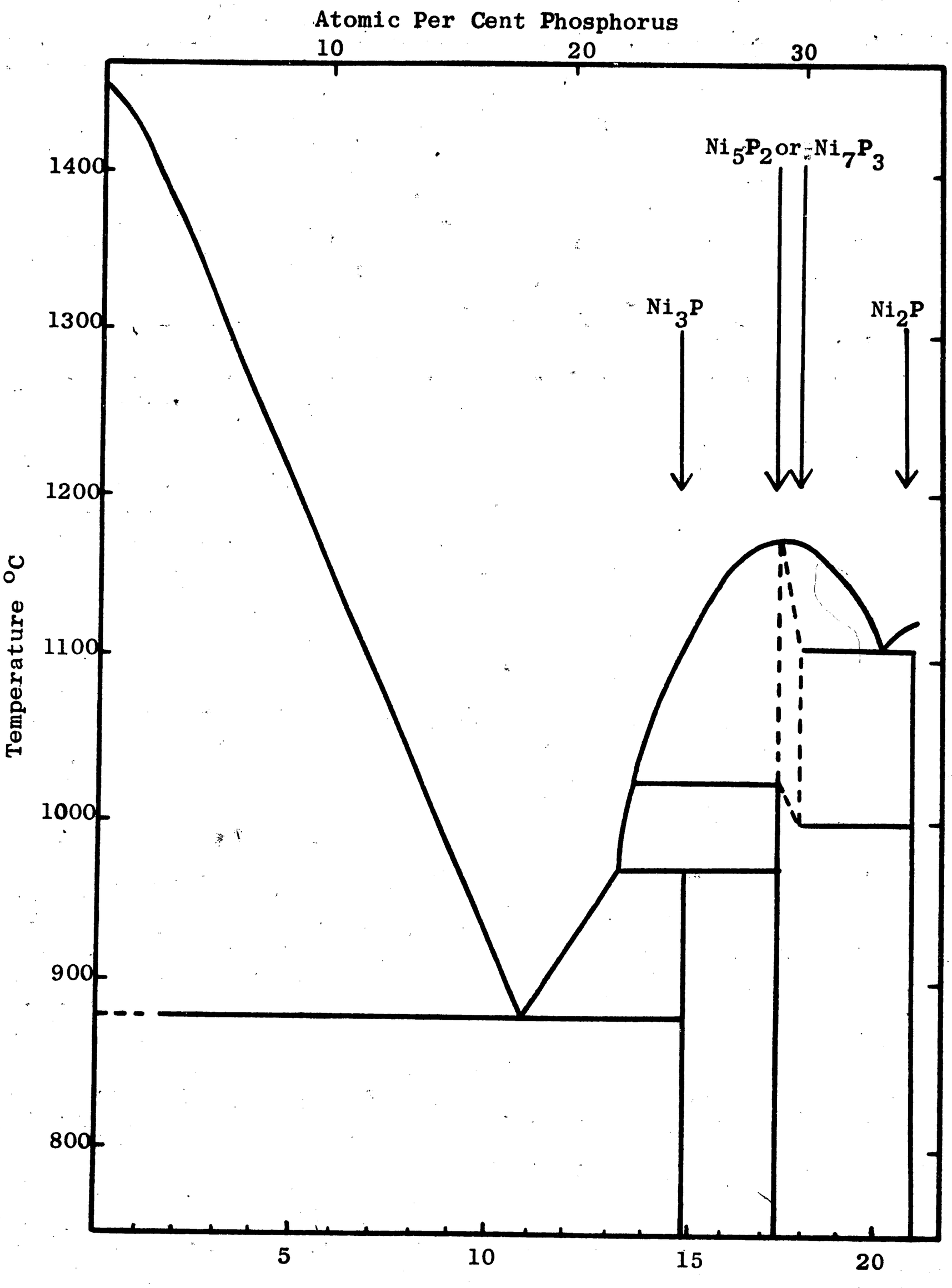

Figure 1. Nickel-Phosphorus Phase Diagram

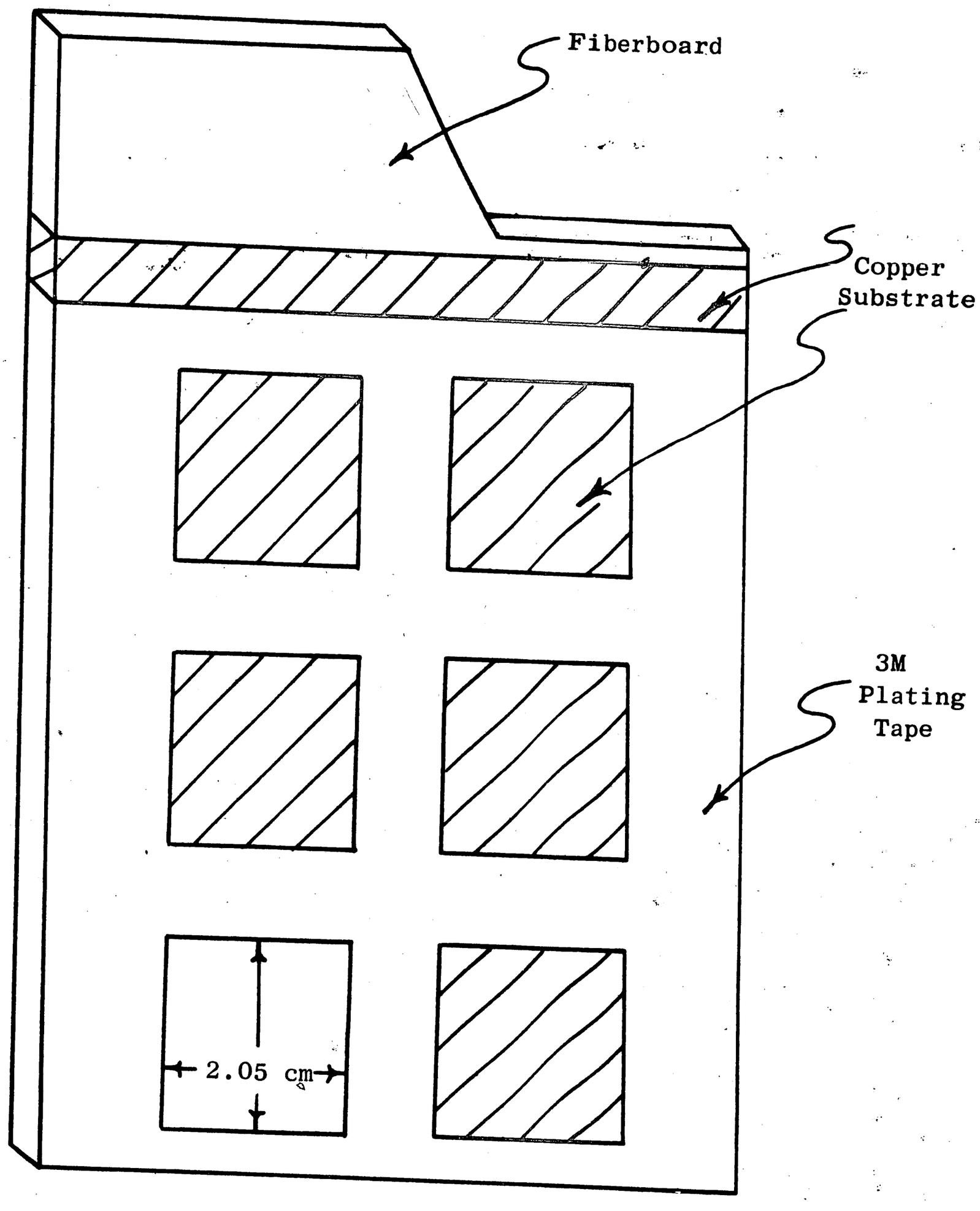

Figure 2. Prepared Cathode

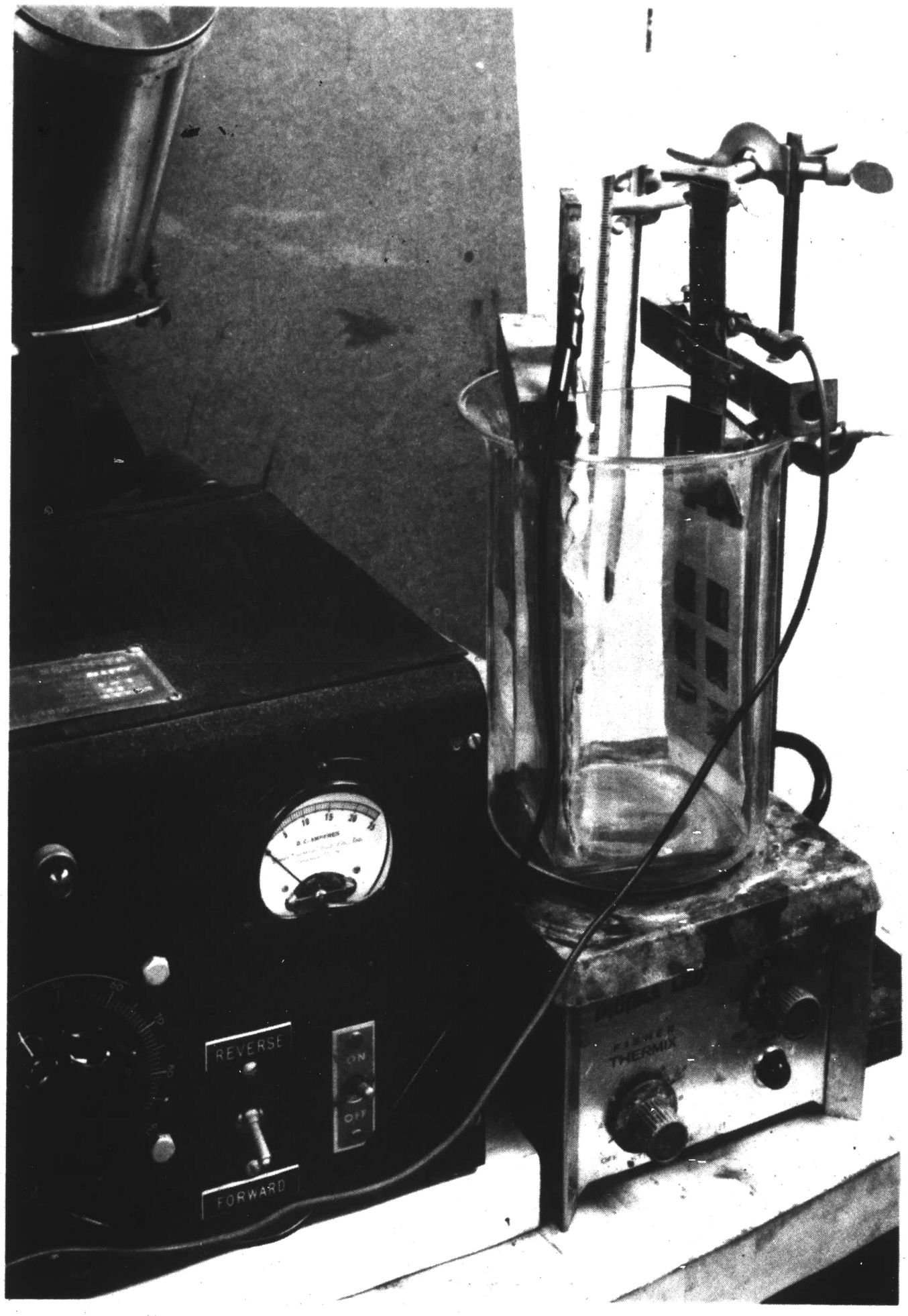

Figure 3. Plating Equipment

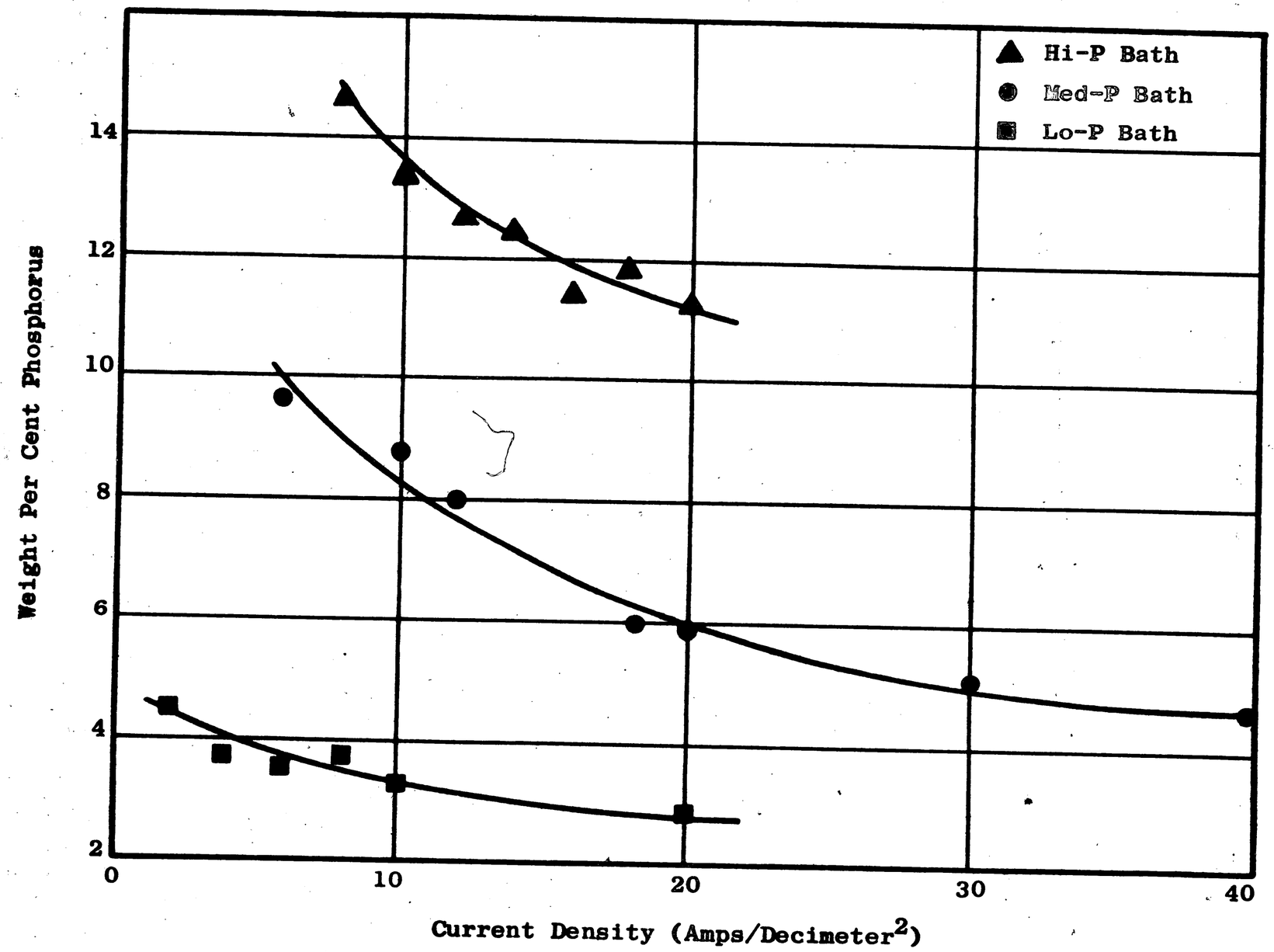

Figure 4. Plot of Alloy Composition versus Current Density

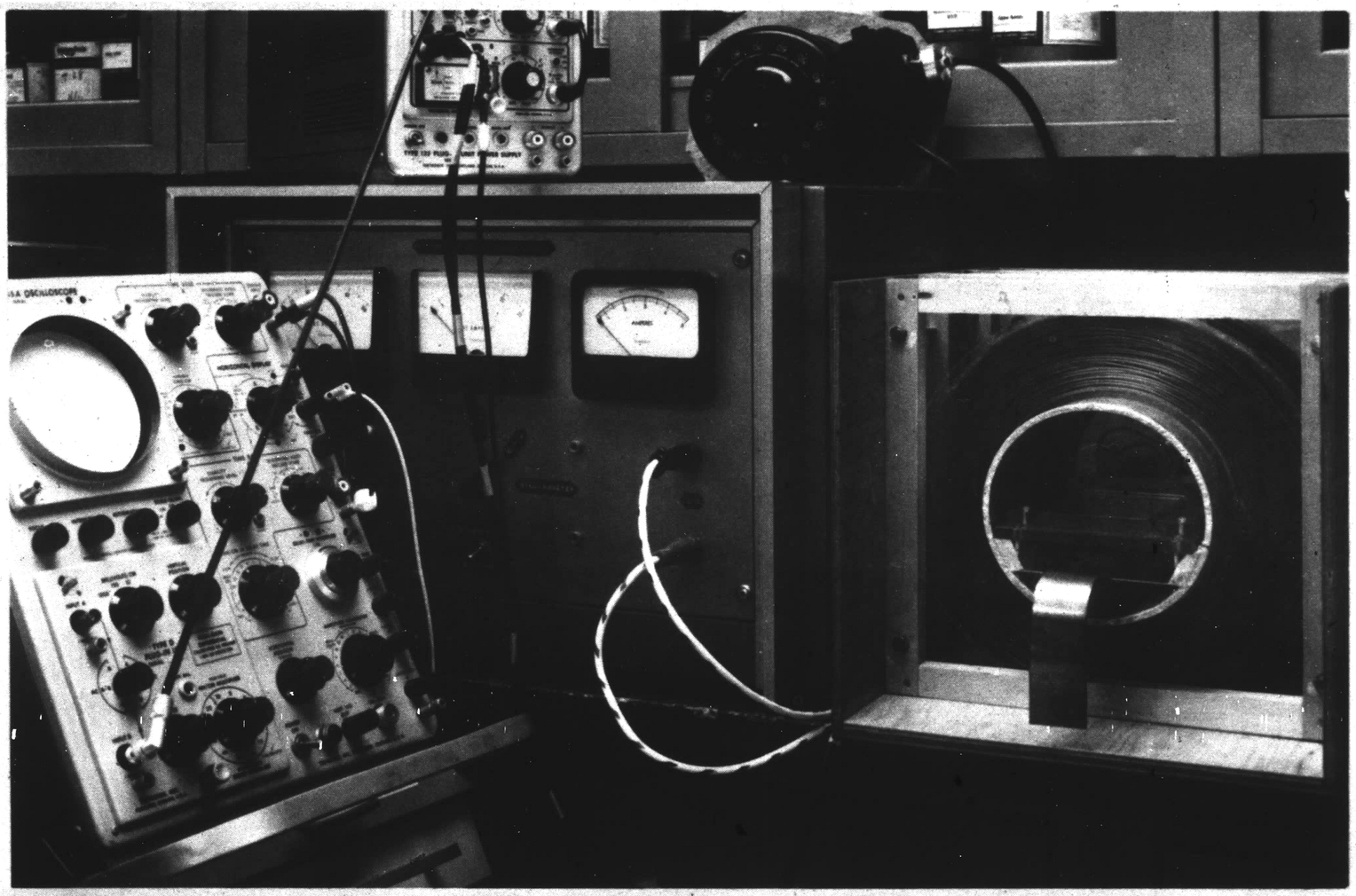

Figure 5. Oscilloscope, Power Supply and Helmholtz Coil - Magnetic Test Equipment

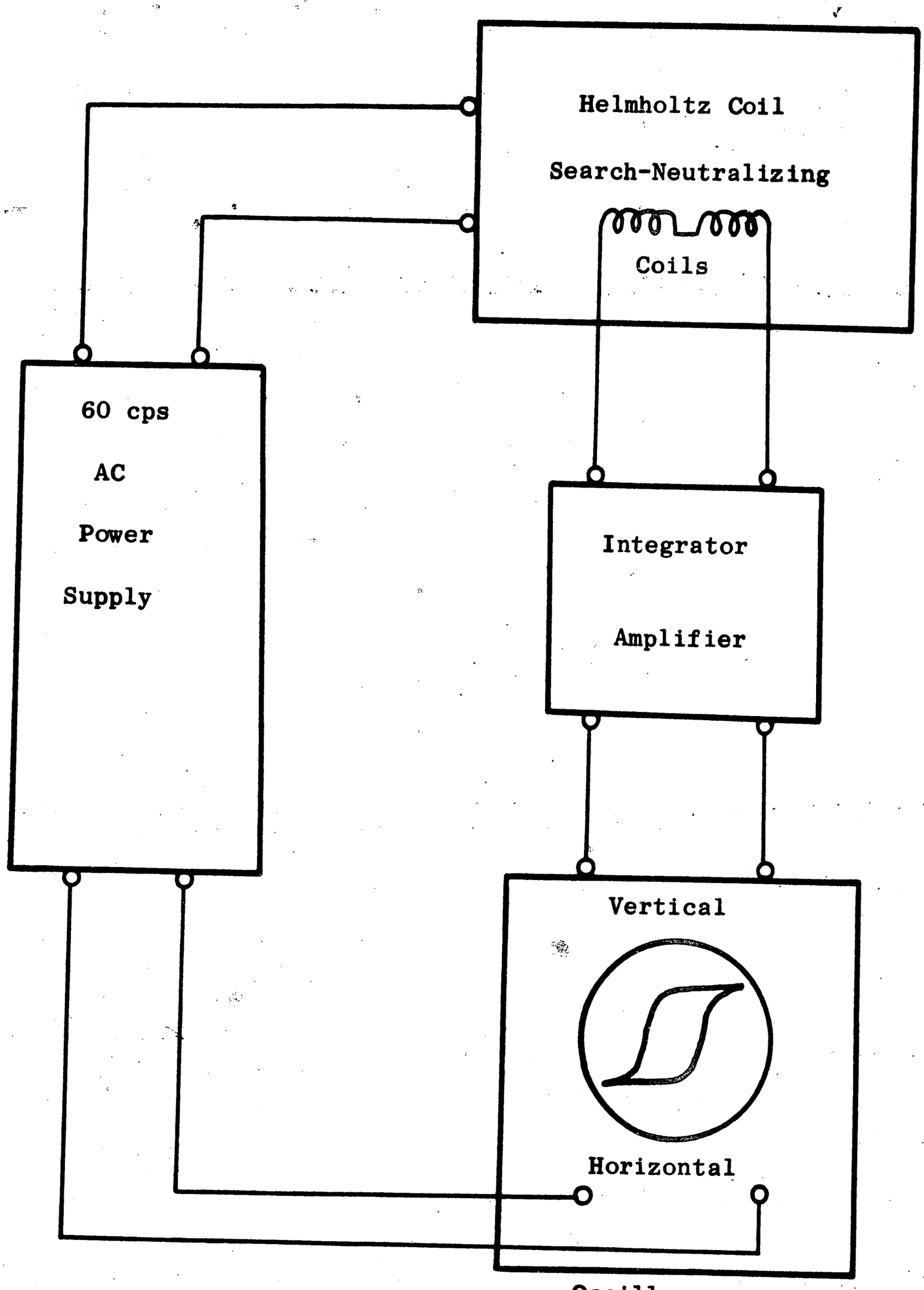

Figure 6 Block Diagram of Hysteresis Looper

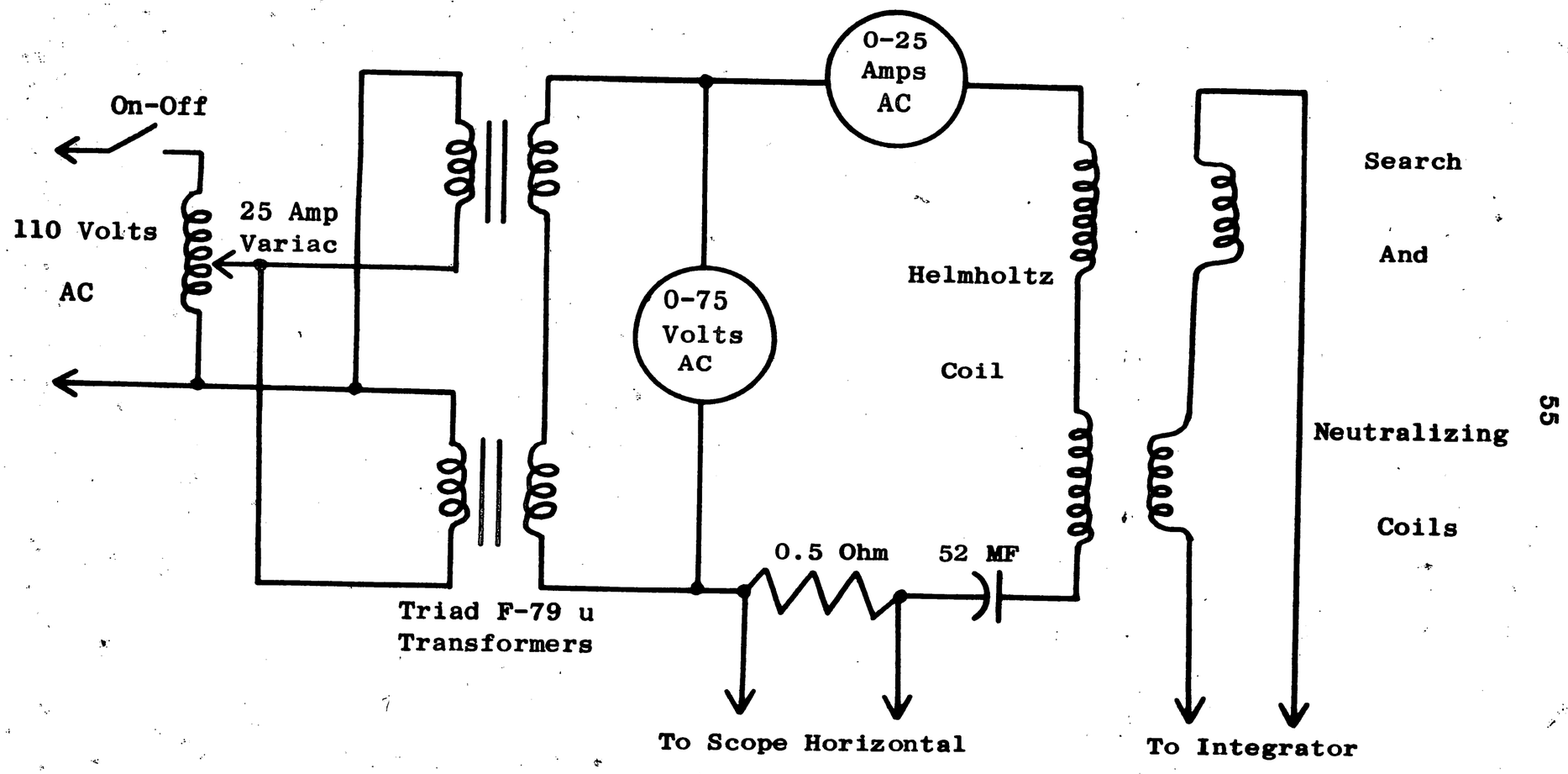

Figure 7 Hysteresis Looper Schematic

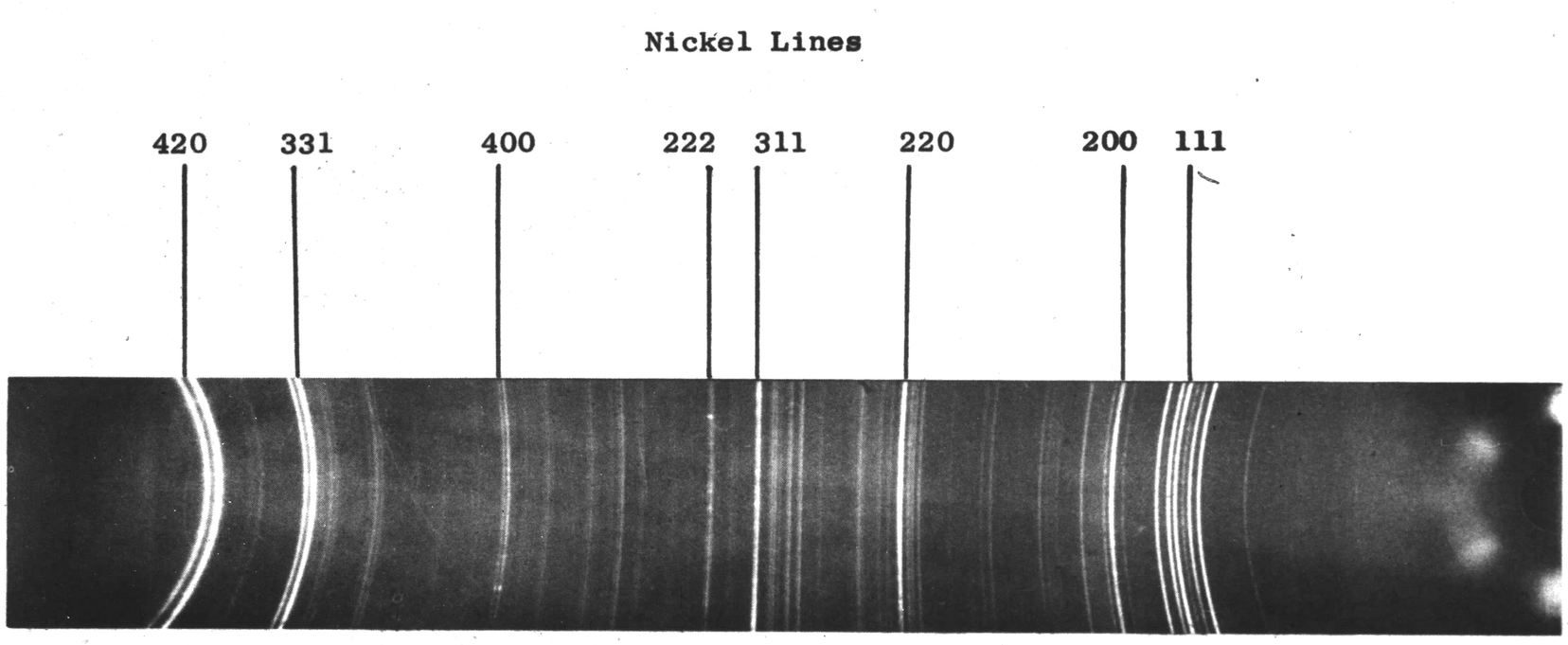

Figure 8. Debye-Scherrer Diffraction Pattern of Less Than 8 w/o P Alloy Heat Treated 4 Hours at 400°C

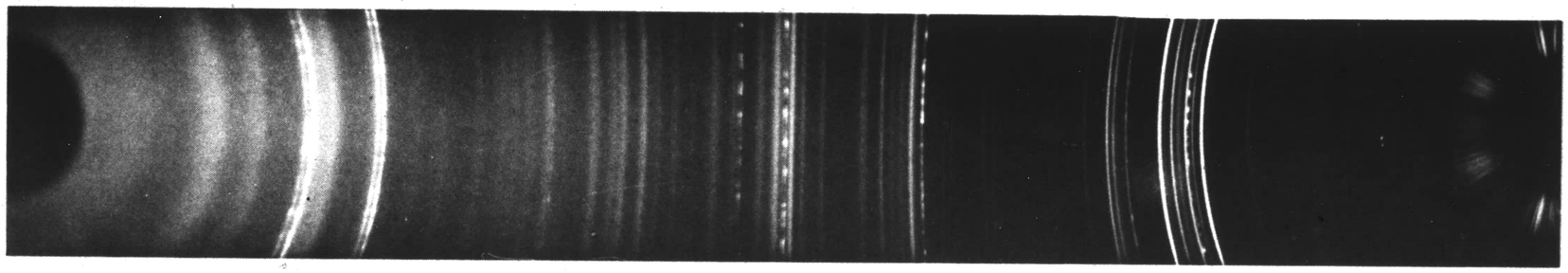

Figure 9. Debye-Scherrer Diffraction Pattern of 8-14 w/o P Alloy Heat Treated 4 Hours at 400°C

Note: Spotty Lines in Both Photos Due to Cu Substrate.

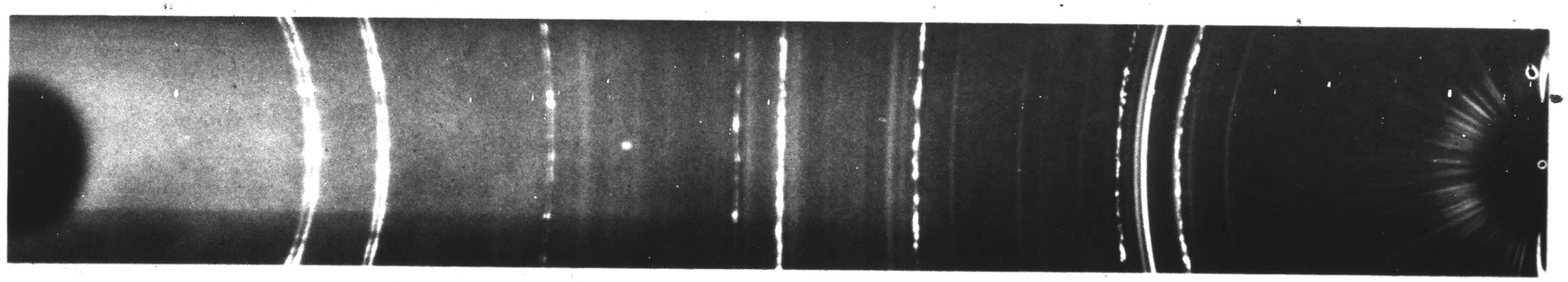

Figure 10. Debye-Scherrer Diffraction Pattern of Greater Than 14 w/o P Alloy Heat Treated 4 Hours at 400°C

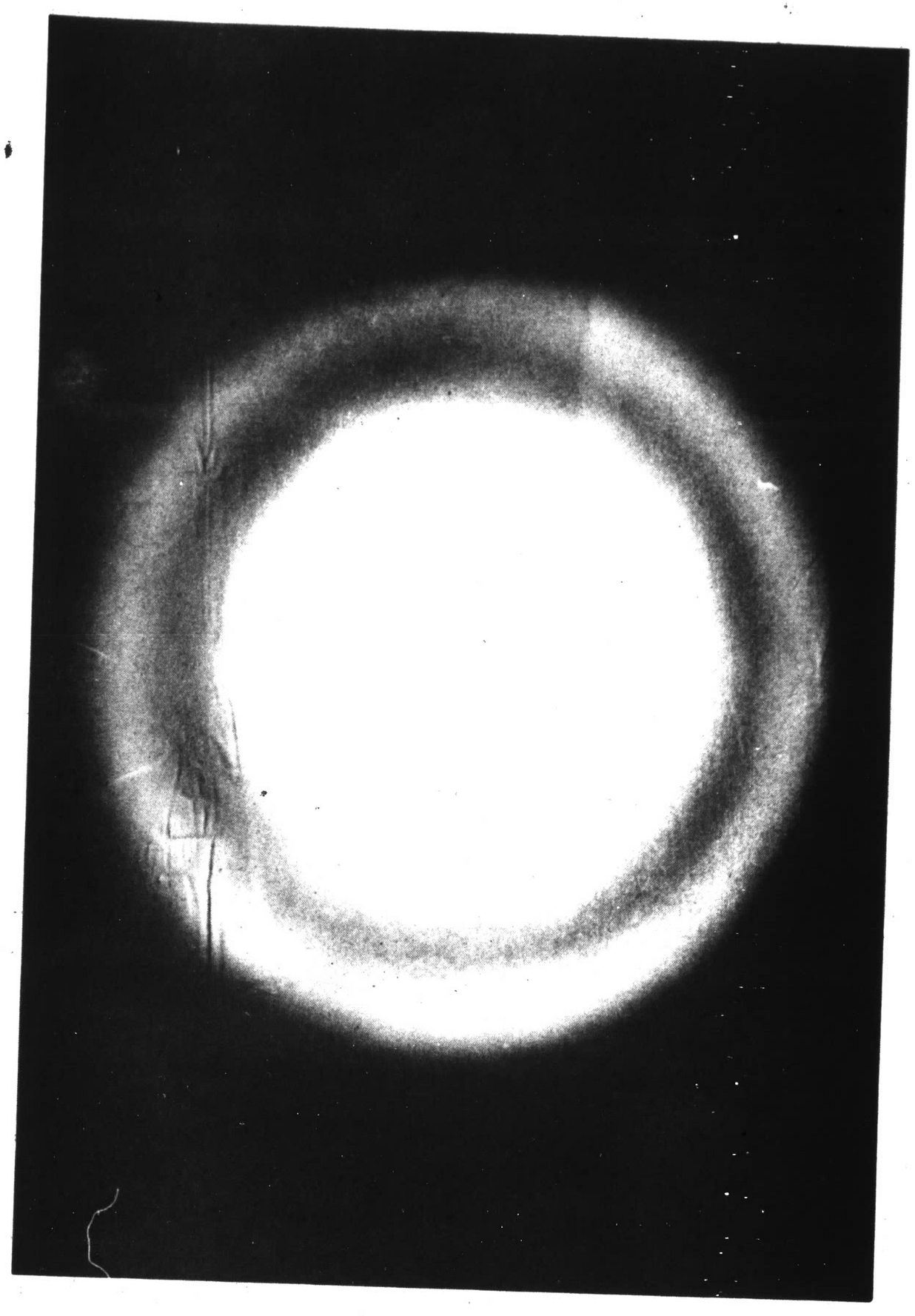

Figure 11. Laue Transmission Pinhole Pattern of 7.6 w/o P As-Plated

Pure Nickel

Figure 11

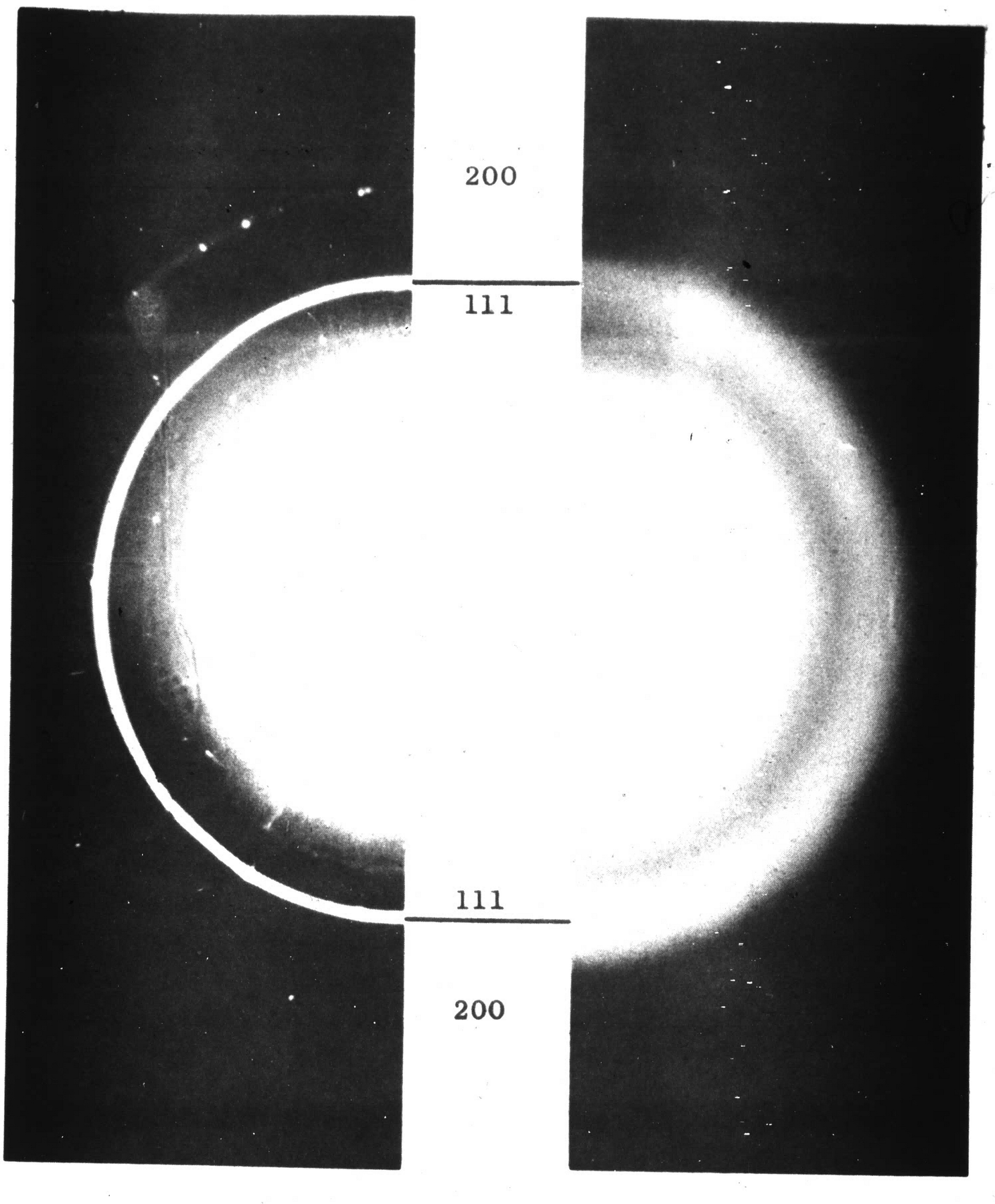

Figure 12. Pure Nickel Compared to Figure 11

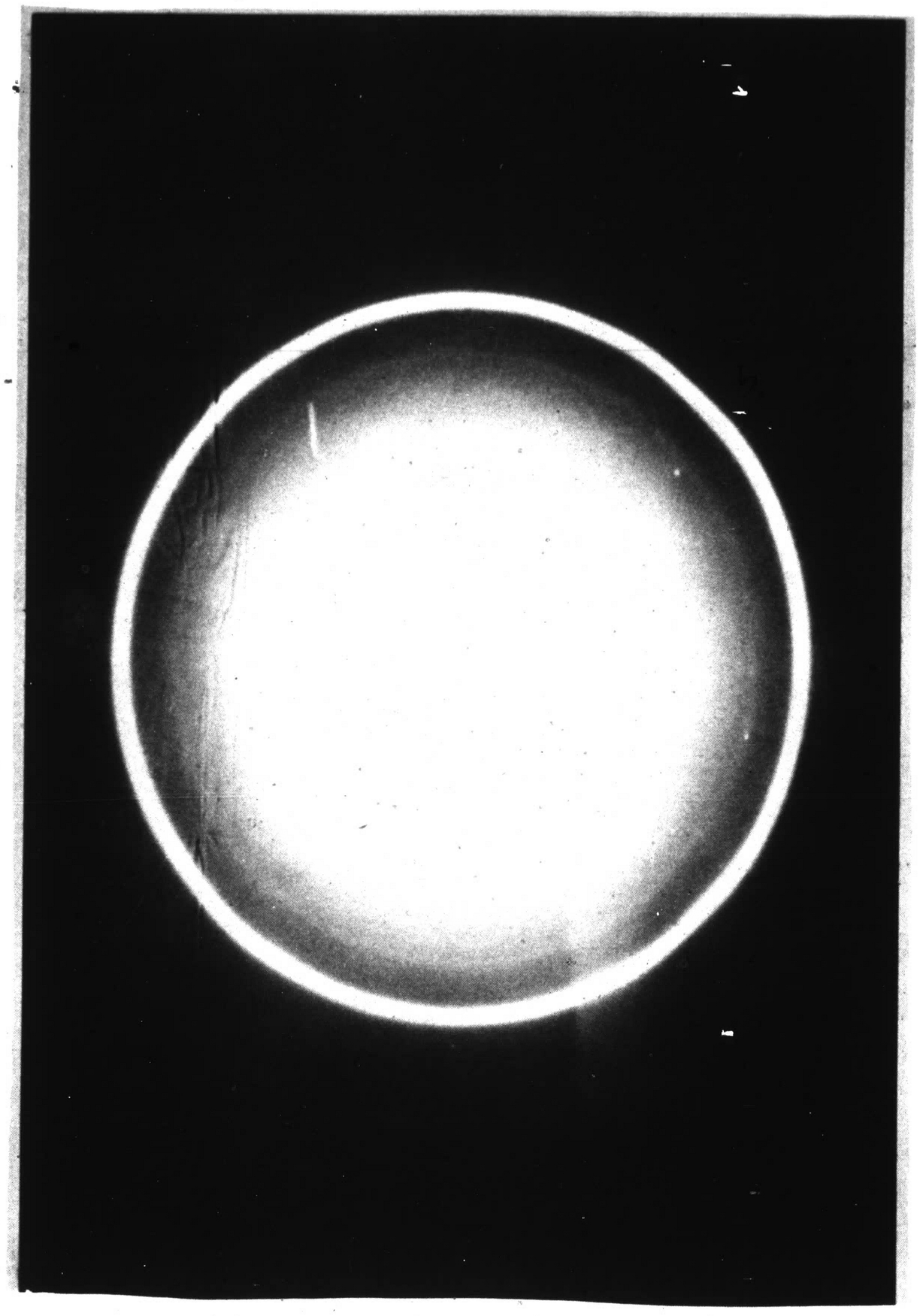

Figure 13. Laue Transmission Pinhole Pattern of 2.9 w/o P Alloy As-Plated

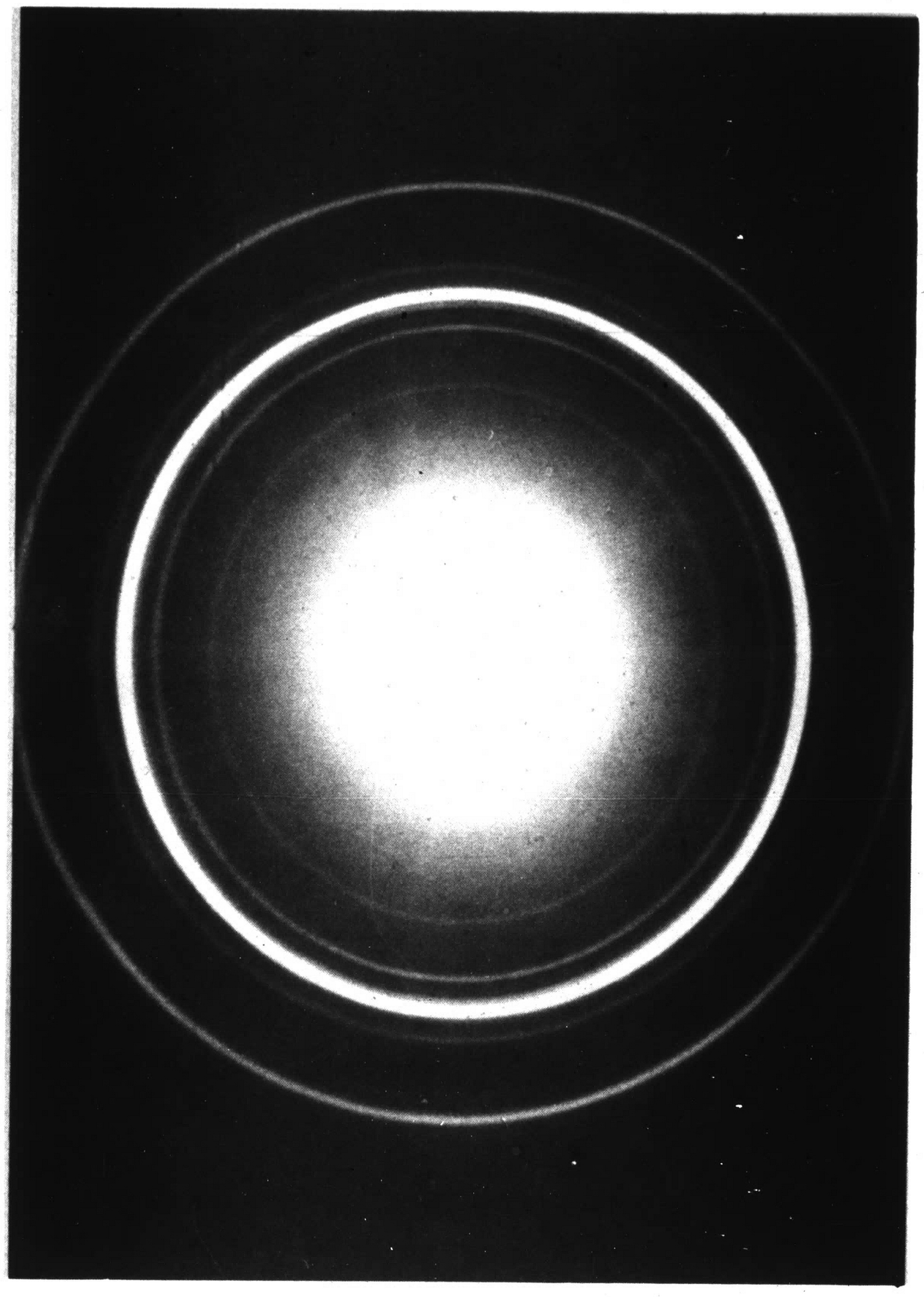

Figure 14. Laue Transmission Pinhole Pattern of 9.6 w/o P Alloy Heat Treated 5 Minutes at 400°C

7.6 w/o P

11.3 w/o P

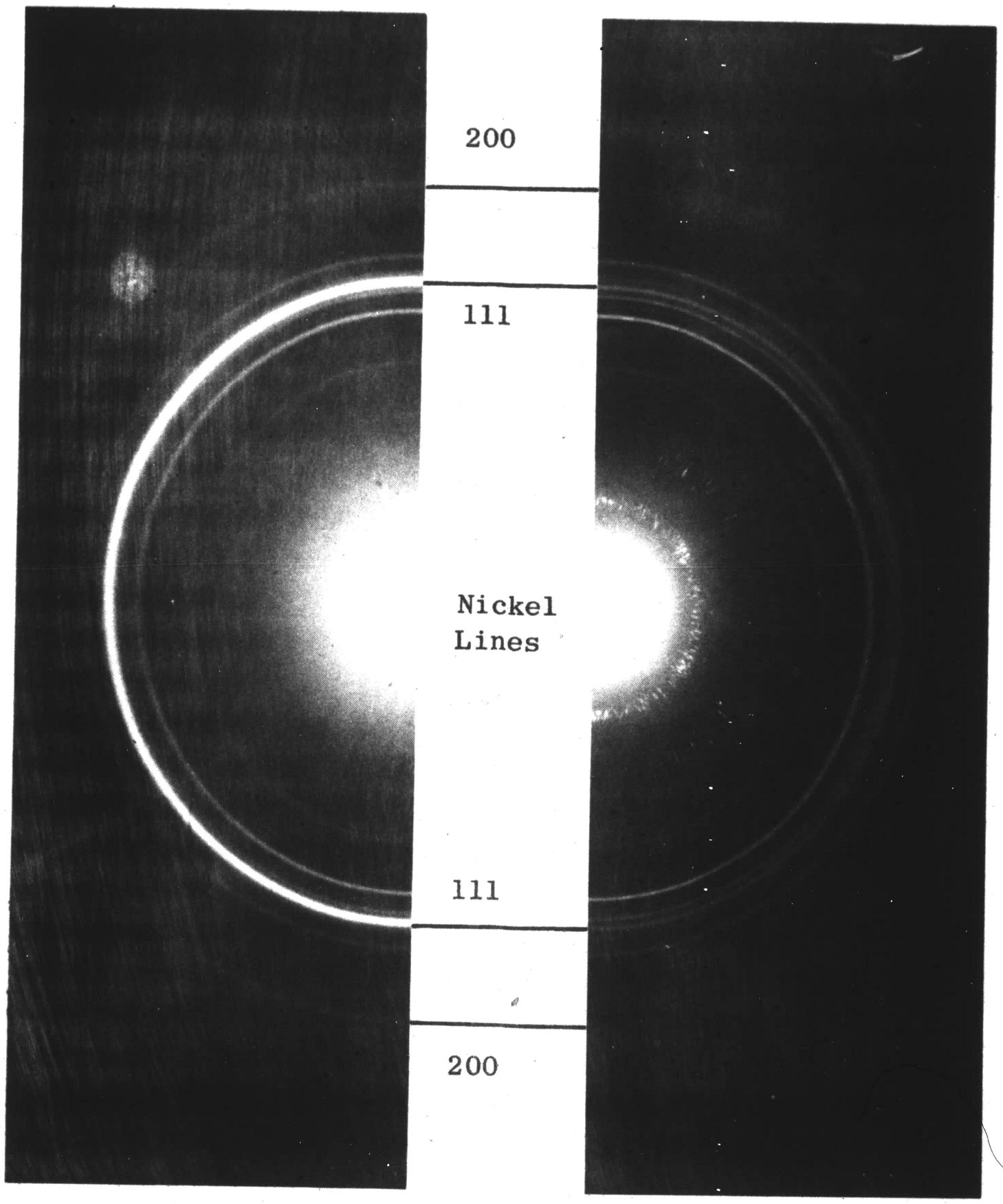

Figure 15. Comparison Between Laue Transmission Pinhole Patterns of 7.6 w/o P and 11.3 w/o P Alloys Both Heat Treated 3 Hours at 400°C

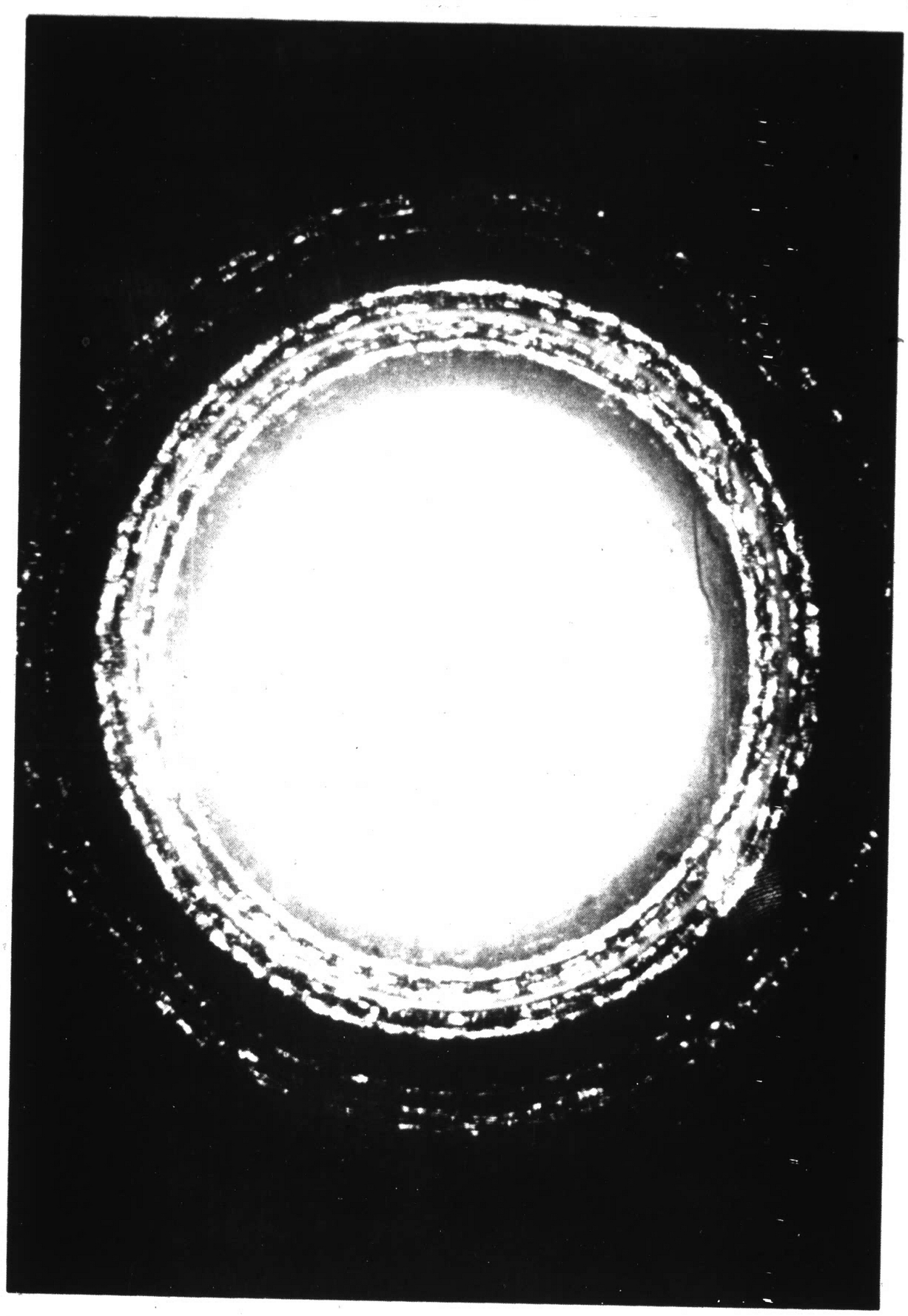

Figure 16. Laue Transmission Pinhole Pattern of 11.0 w/o P Alloy Heat Treated 3 Hours at 400°C. Note: Solid Rings of Nickel 111 and 200 can be Seen

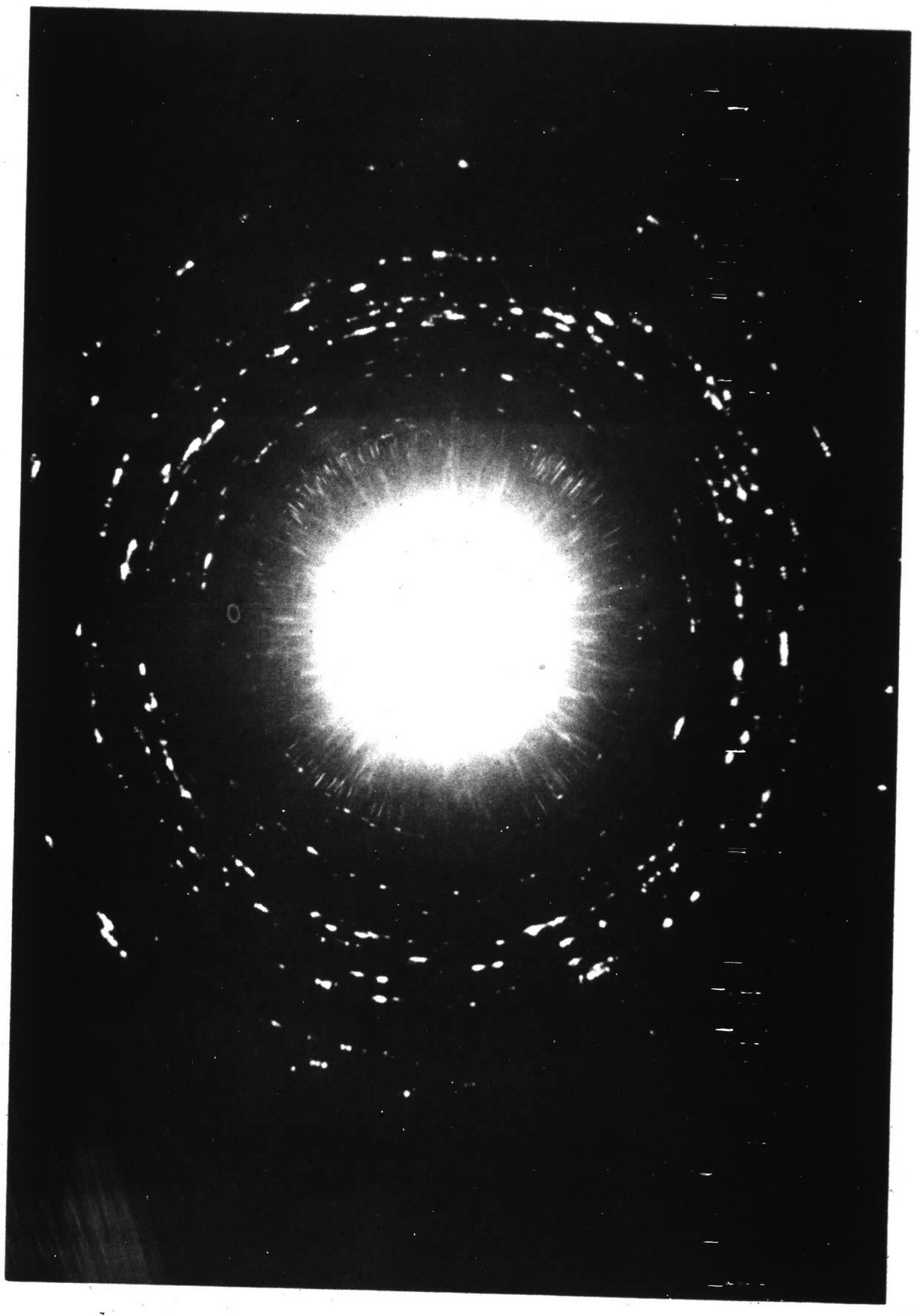

Figure 17. Laue Transmission Pinhole Pattern of 14.0 w/o P Alloy Heat Treated 3 Hours at 400°C

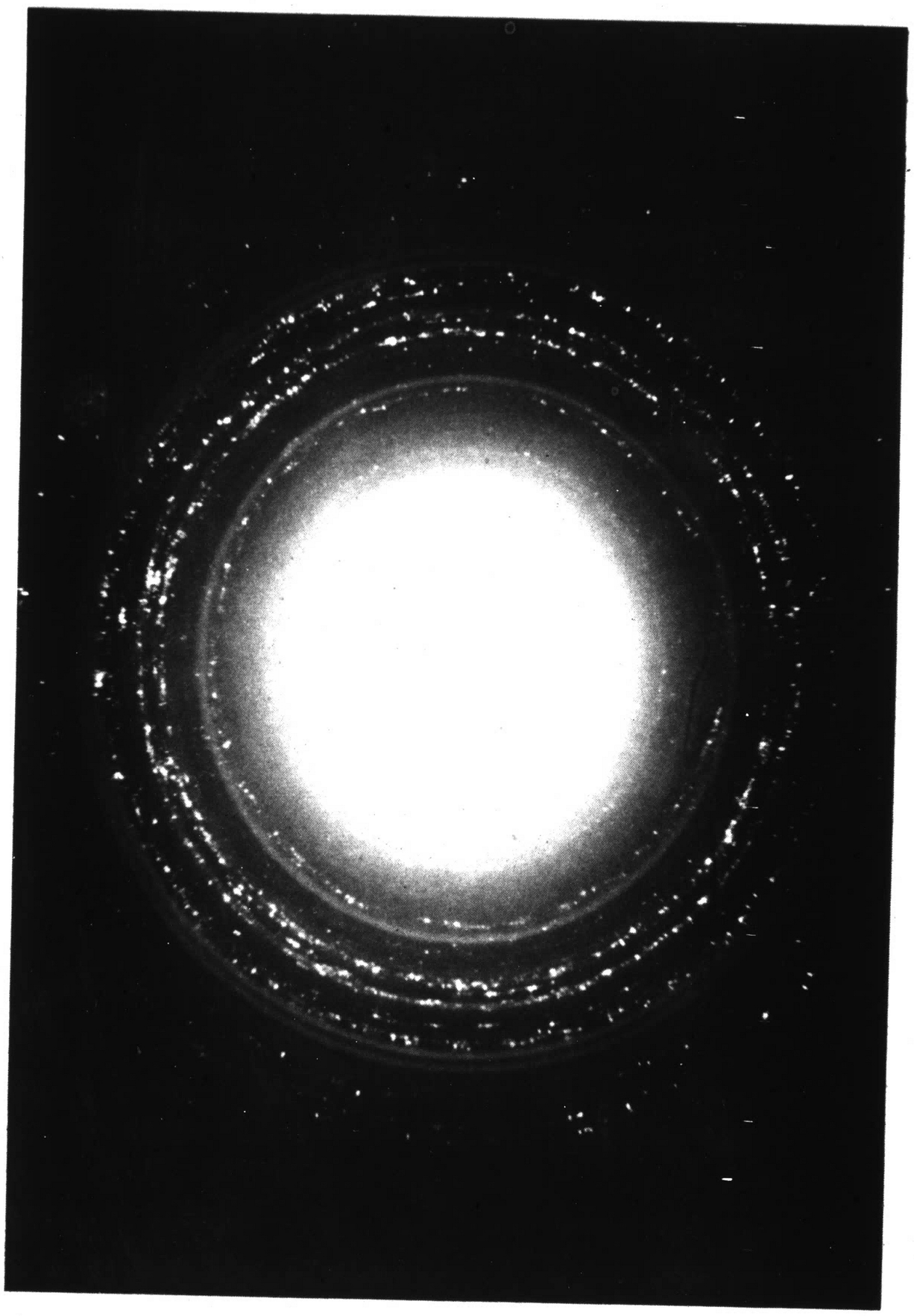

Figure 18. Laue Transmission Pinhole Pattern of 14.8 w/o P Alloy Heat Treated 3 Hours at 400°C

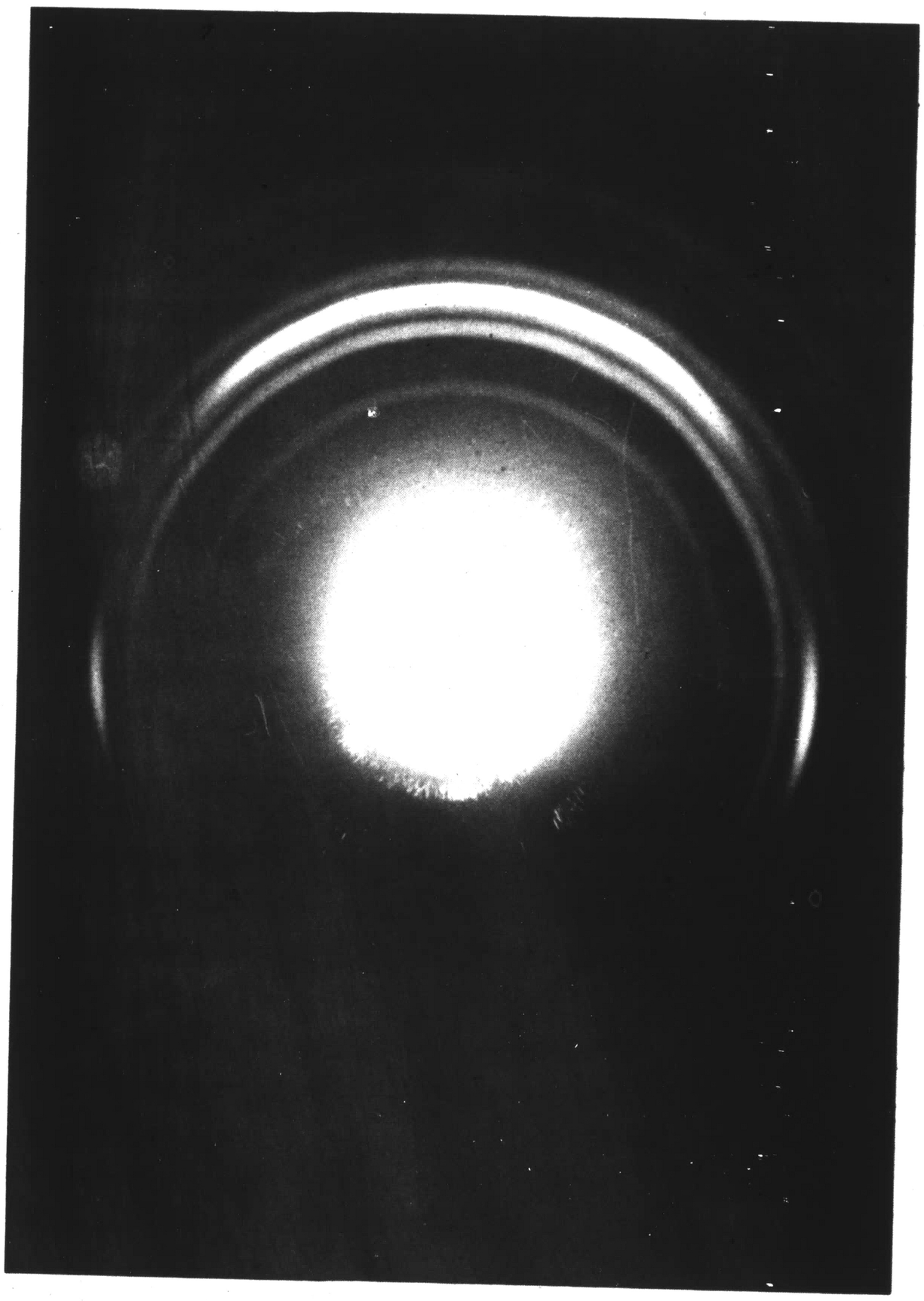

Figure 19. Orientation Laue Pinhole Pattern of 9.1 w/o P Alloy Heat Treated 3 Hours at 400°C

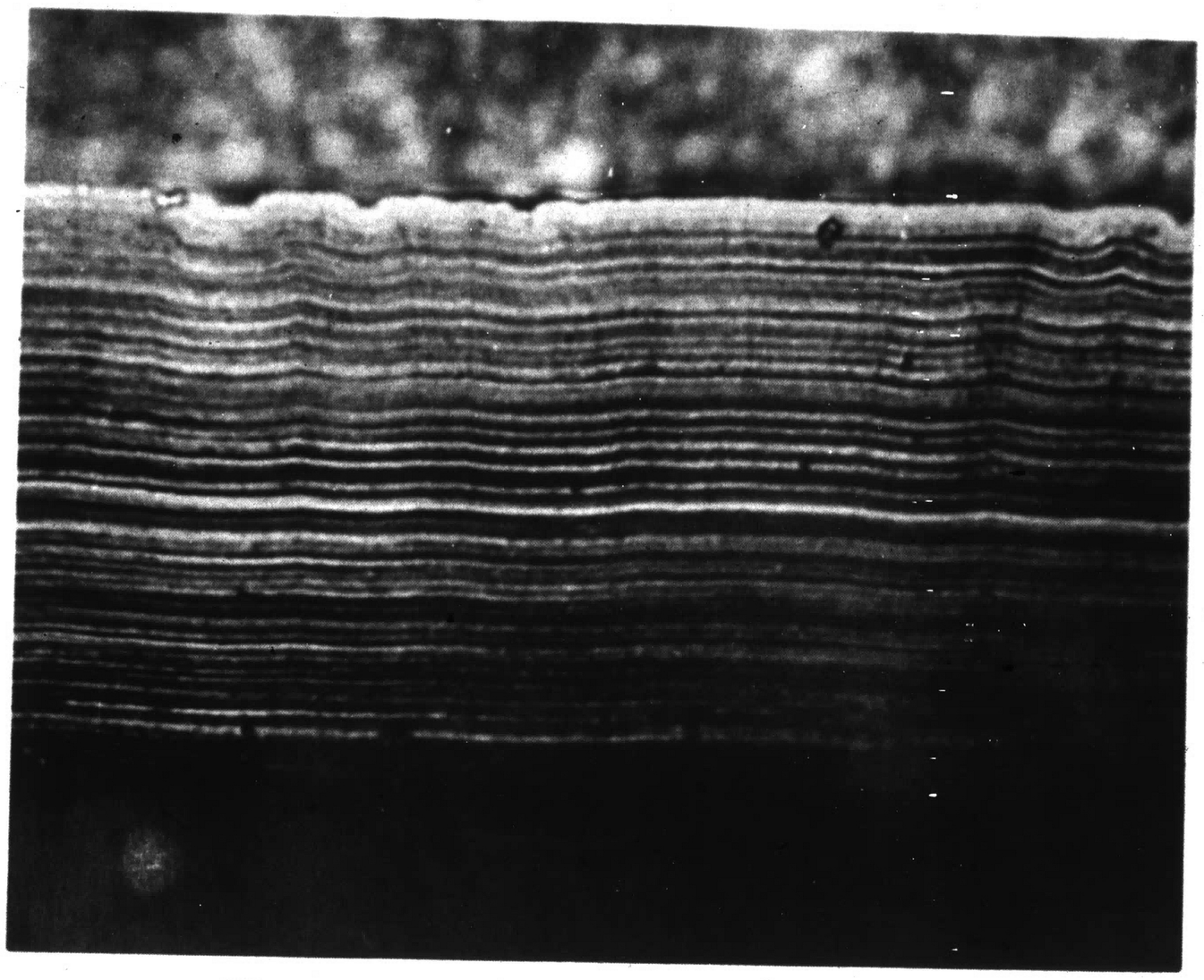

Figure 20. Lamellar Structure of
8.7 w/o P Alloy Heat Treated
1 Hour at 400°C (700X)

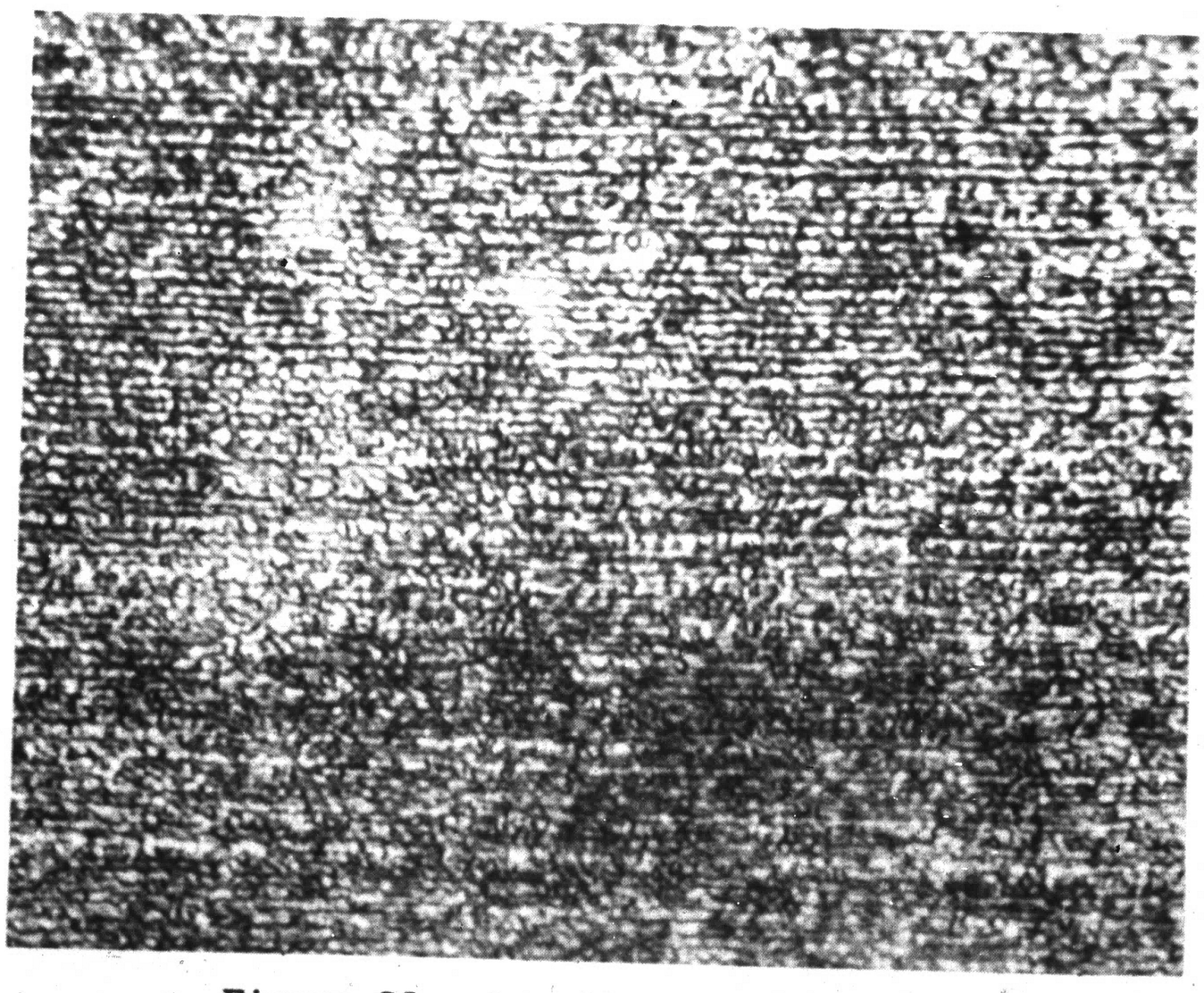

Figure 21. Lamellar Structure of
8.7 w/o P Alloy Heat Treated
1 Hour at 700°C (700X)

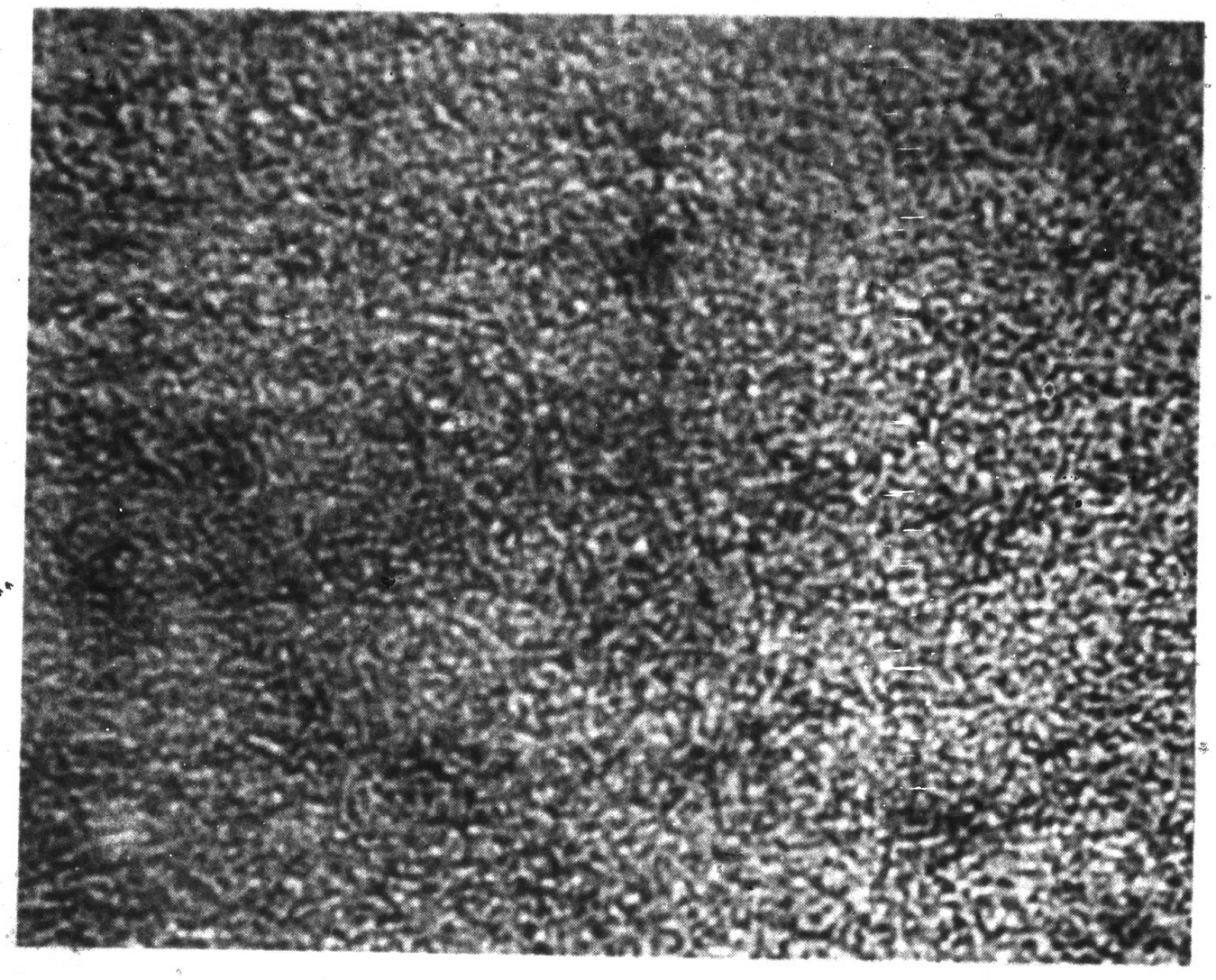

Figure 22. Top View of Ni_3P Precipitate in 9.7 w/o P Alloy Heat Treated 3 Hours at 450°C (700X)

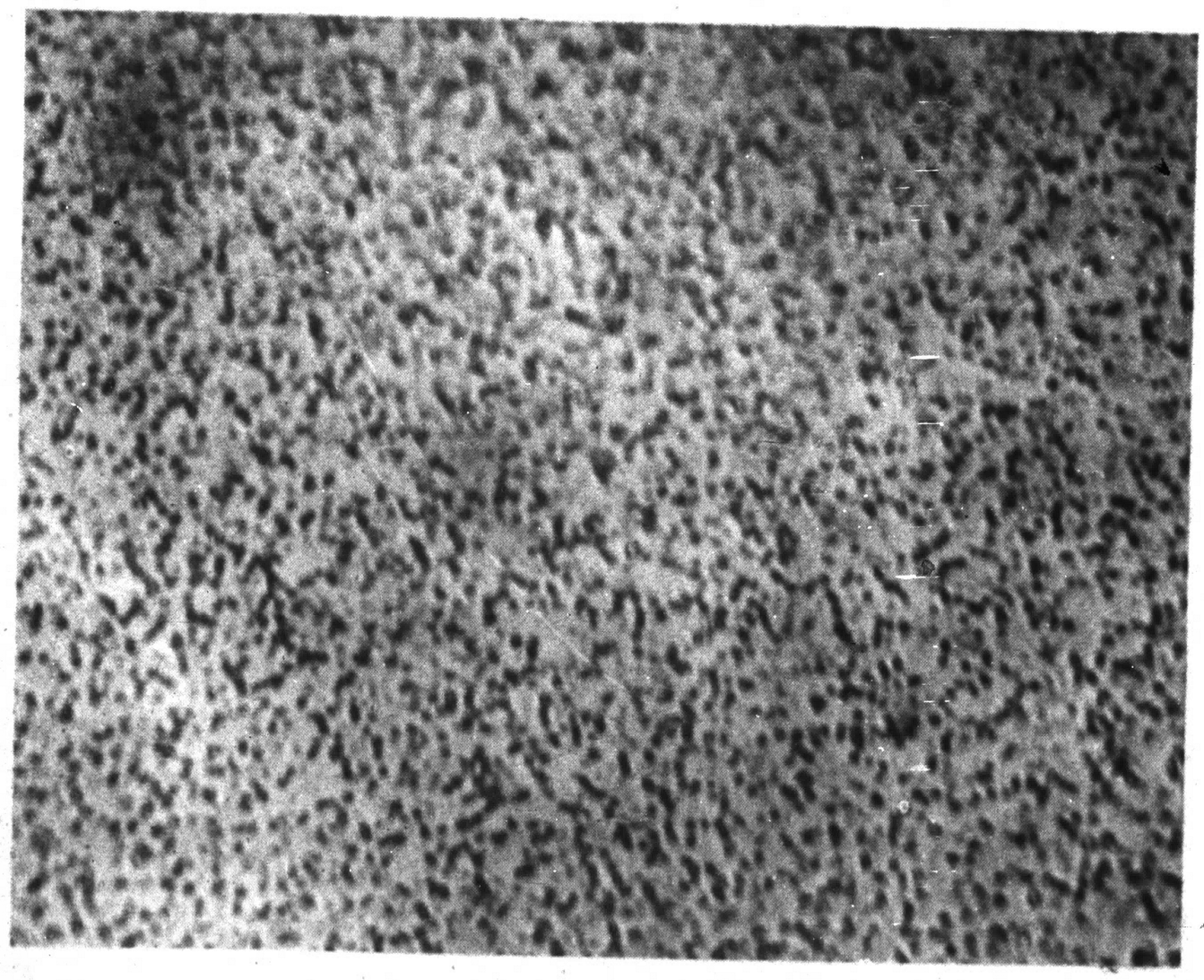

Figure 23. Top View of Ni_3P Precipitate in 9.7 w/o P Alloy Heat Treated 3 Hours at 700°C (700X)

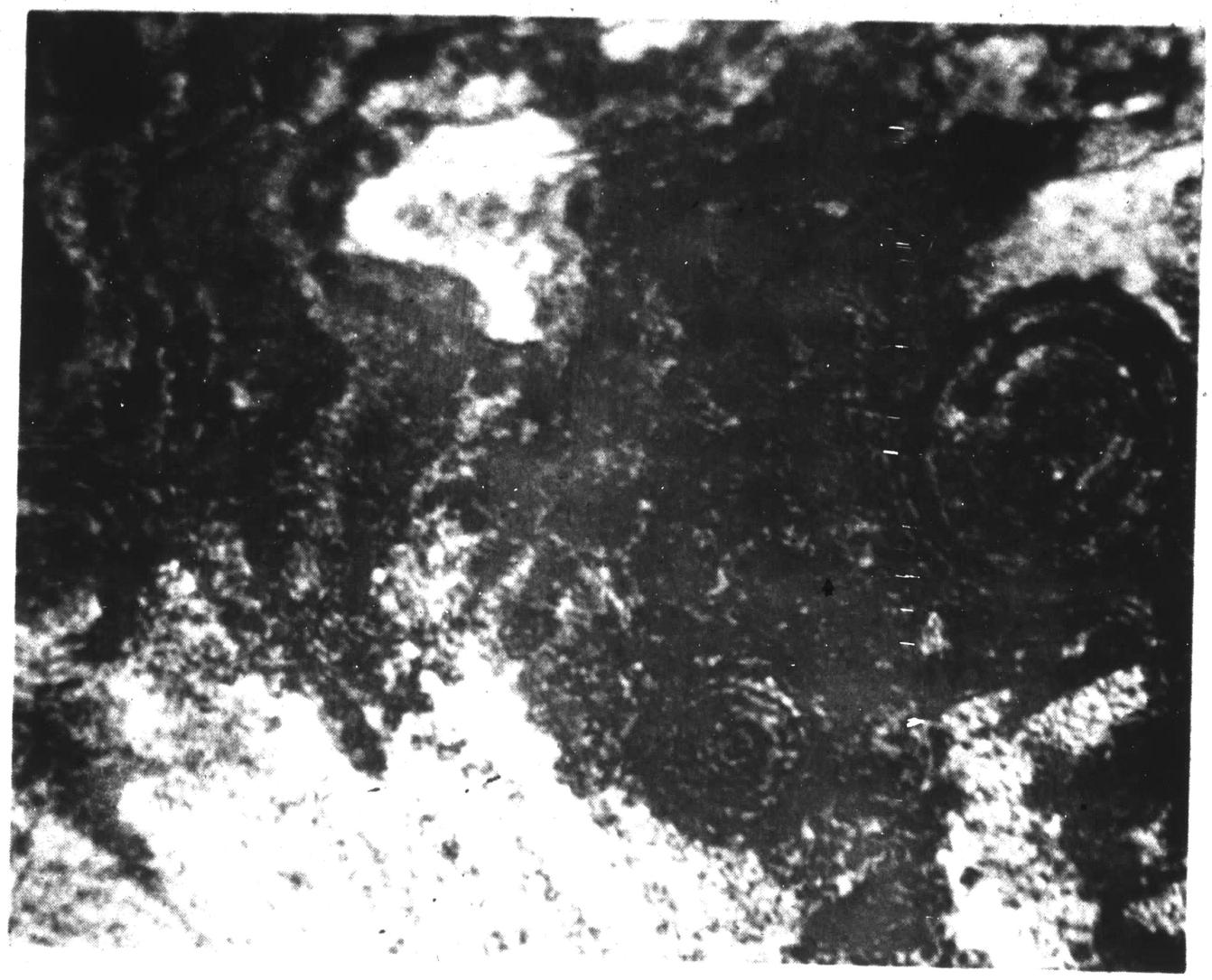

Figure 24. Top View Showing Sheet Structure of Ni-Ni_3P in 8.3 w/o P Alloy Heat Treated 1 Hour at 450°C (700X)

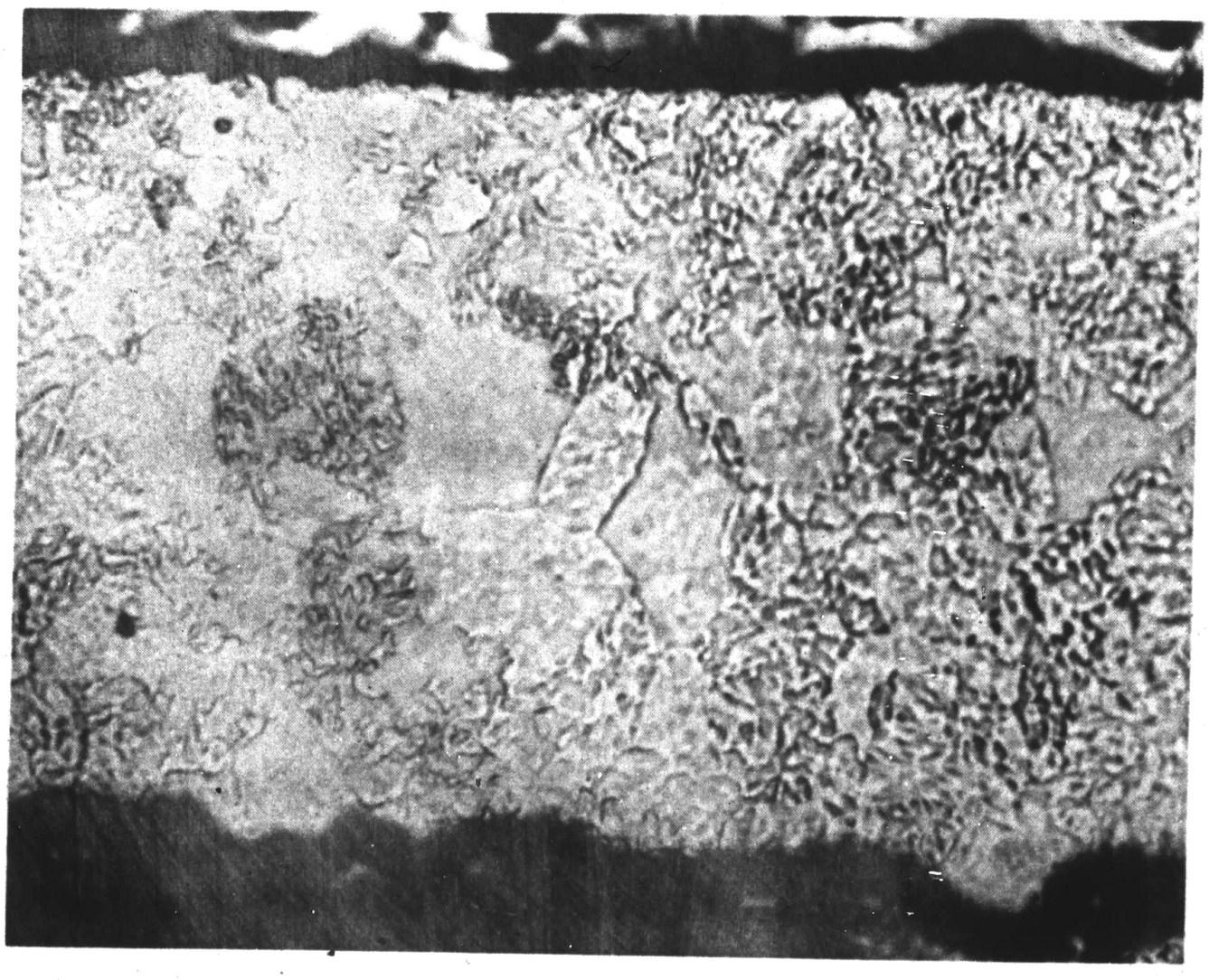

Figure 25. Large Grain Structure of High Phosphorus Alloys Seen in 14.3 w/o P Alloy Heat Treated 1 Hour at 700°C (700X)

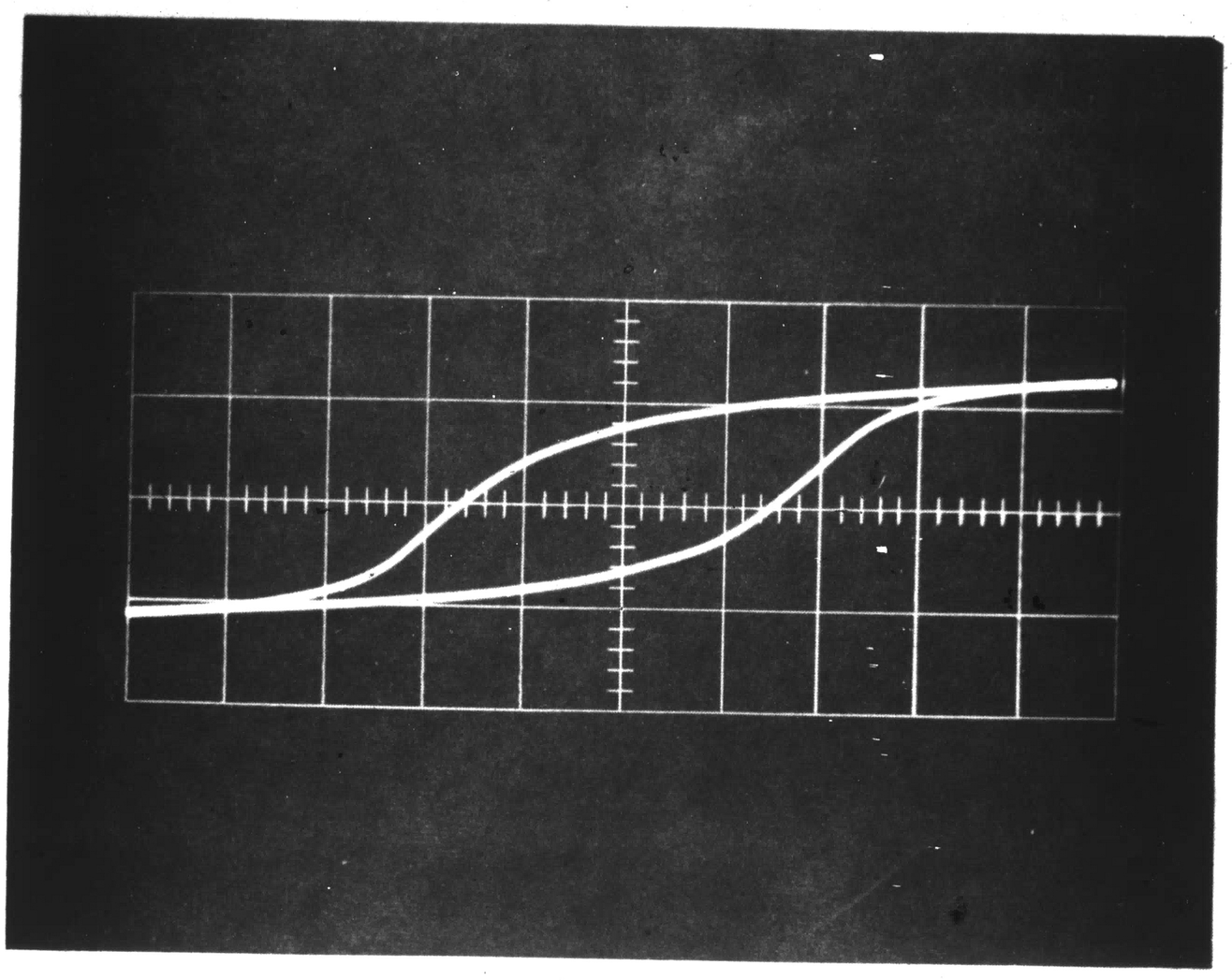

Figure 26. Hysteresis Loop of As-Plated Pure Nickel

Figure 27. Hysteresis Loop of As-Plated 1.5 w/o P Alloy

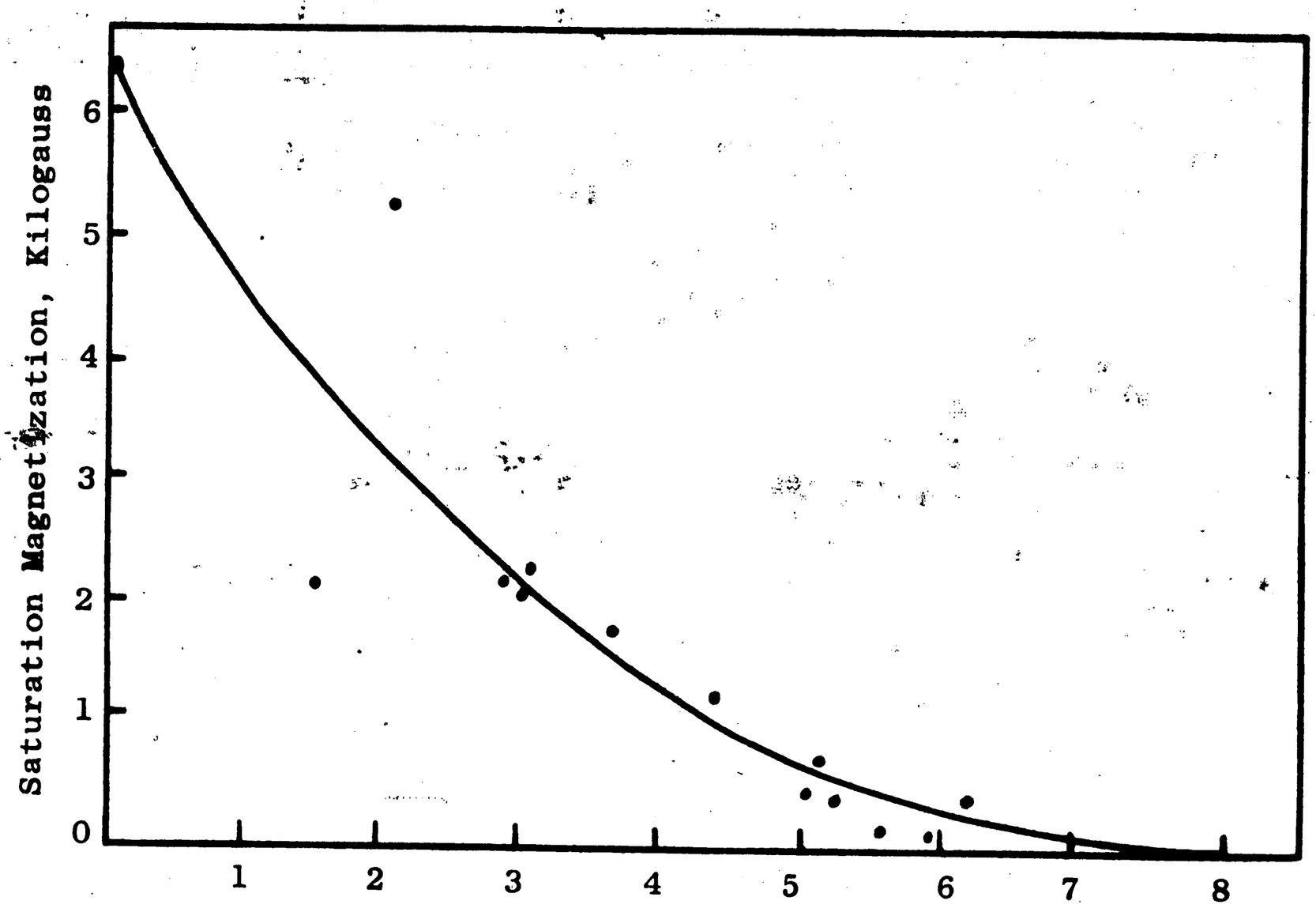

Figure 28. Plot of Ms versus Composition in As-Plated Alloys

Figure 29. Plot of Hci versus Composition in As-Plated Alloys Stress Relief Annealed for 4 Hours at 200°C

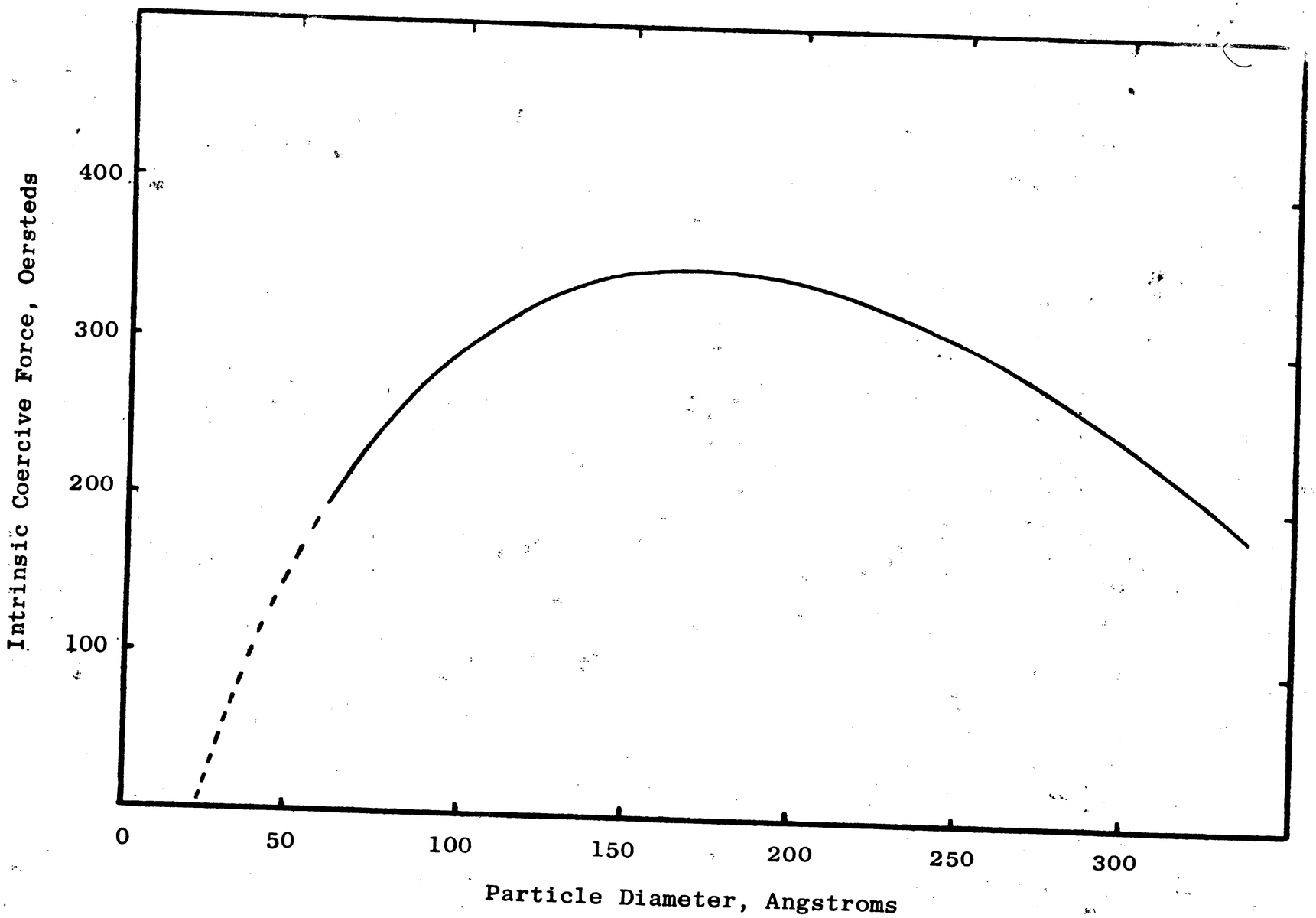

Figure 30. Schematic Relationship of Intrinsic Coercive Force to Particle Diameter for Typical Ferromagnetic Material

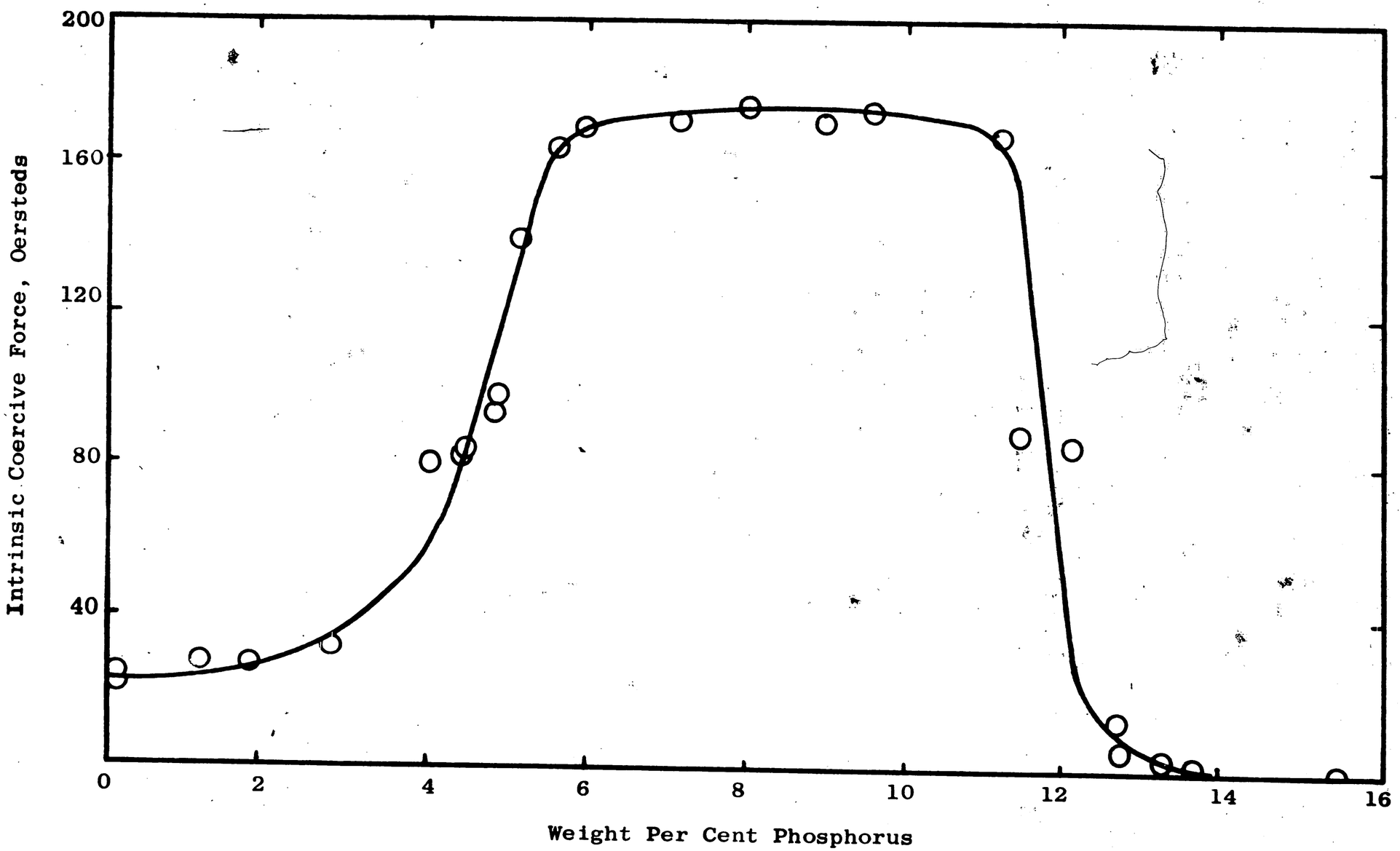

Figure 31. Plot of Hci versus Composition for Alloys Heat Treated 1 Hour at 400°C

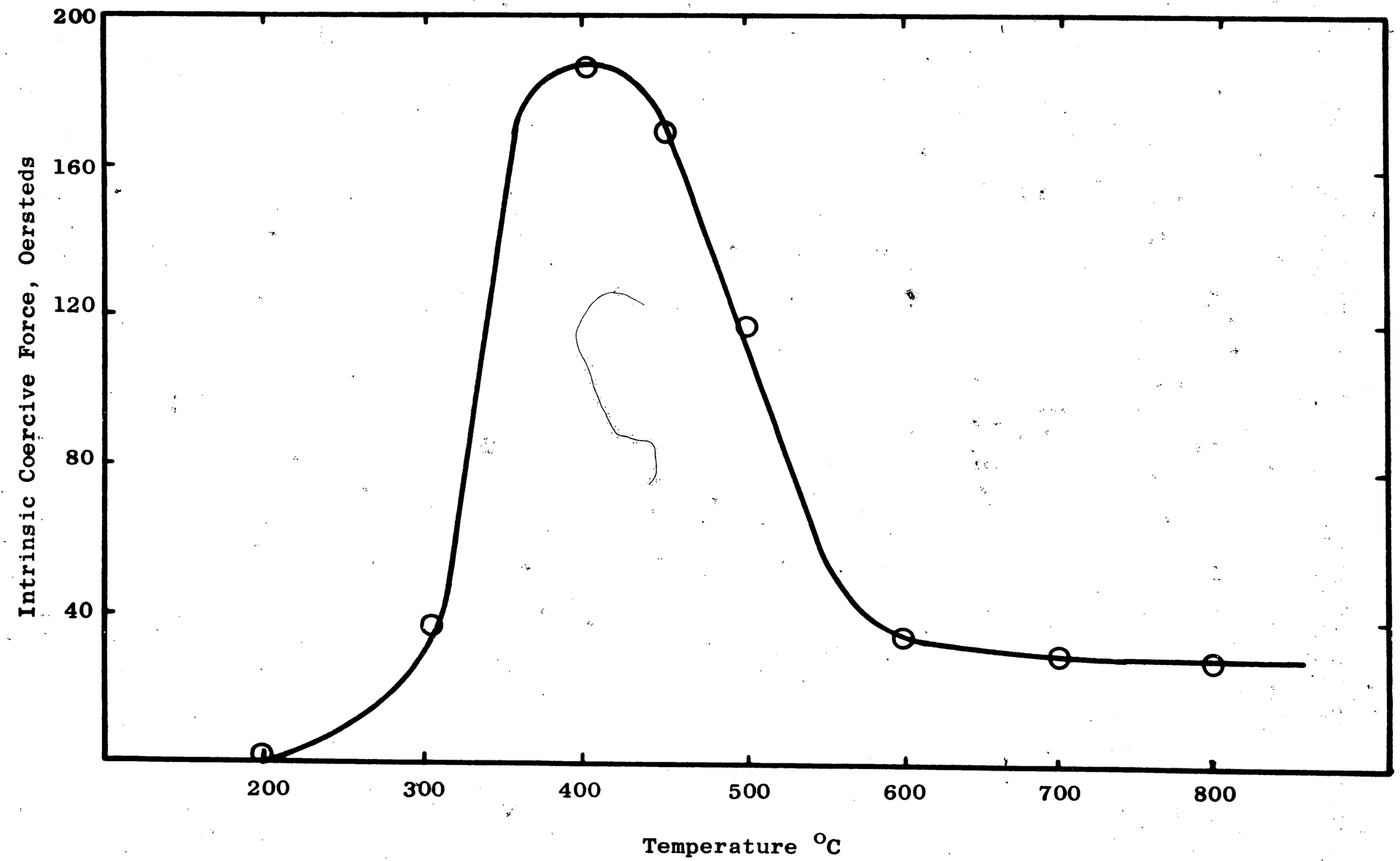

Figure 32. Plot of Hci versus Temperature of 1 Hour Heat Treatment for 9.4 w/o P Alloy

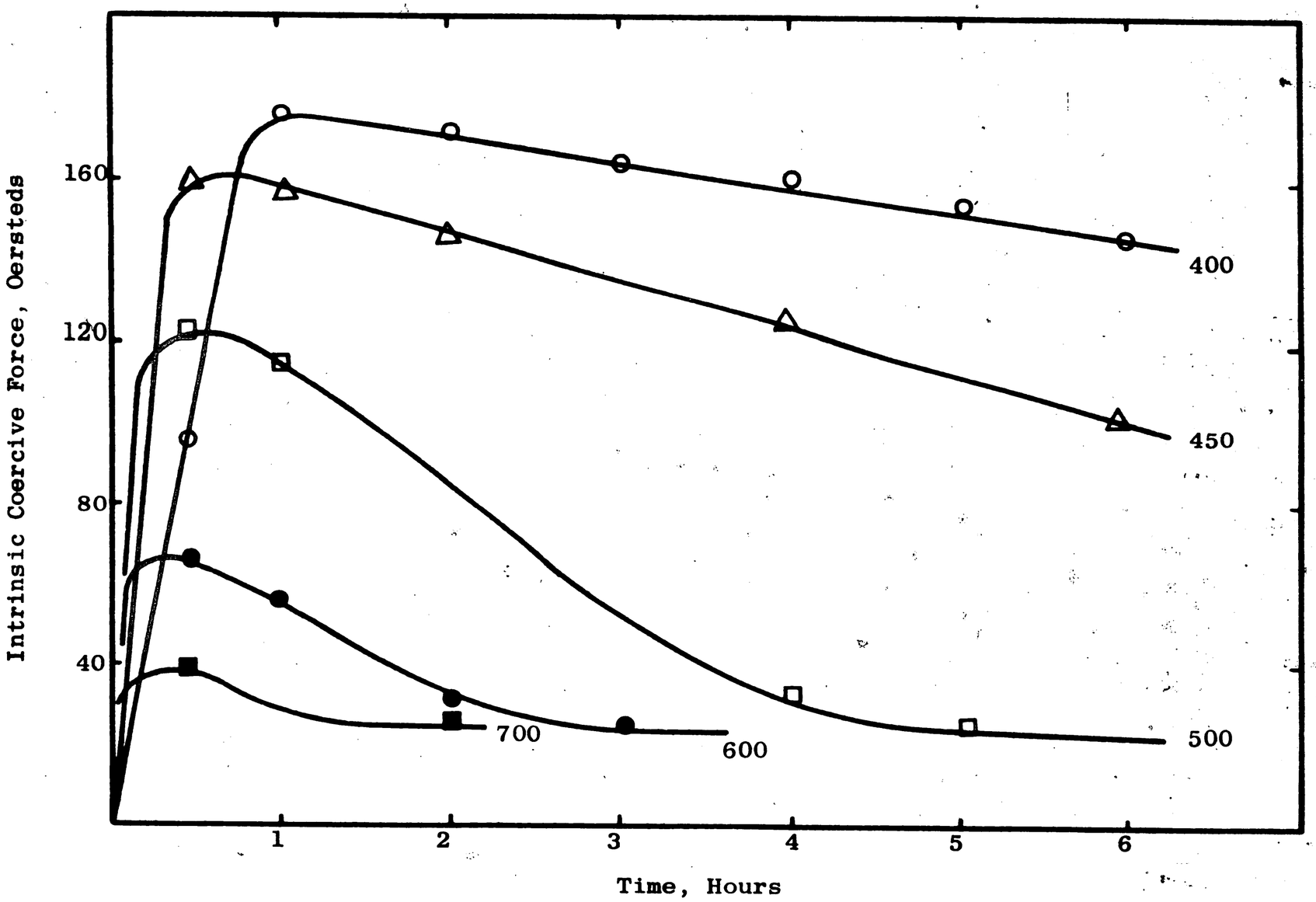

Figure 33. Plot of Hci versus Time at Given Temperature for 9.4 w/o P Alloy

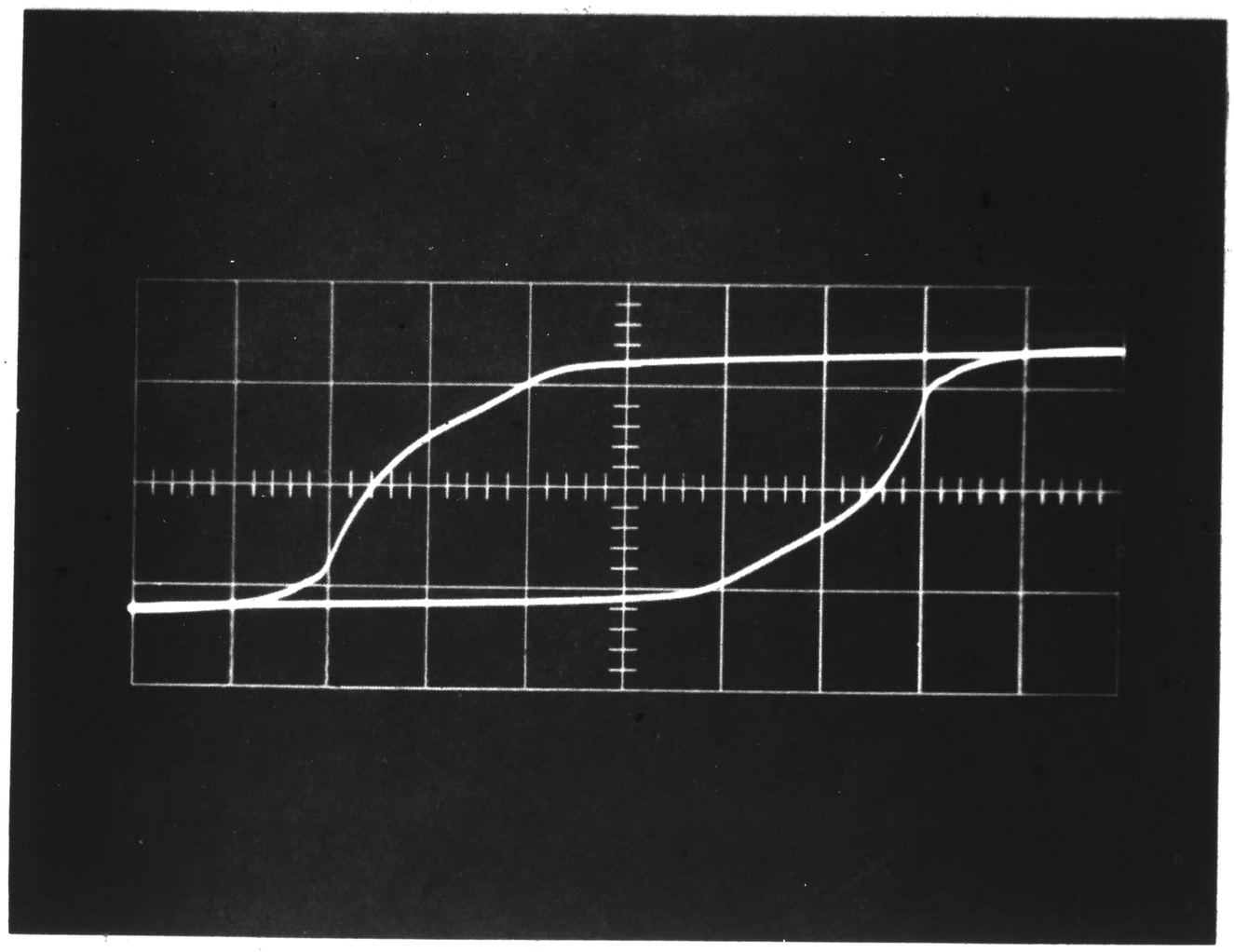

Figure 34. Hysteresis Loop of 7.6 w/o P Alloy Heat Treated 2 Hours at 400°C

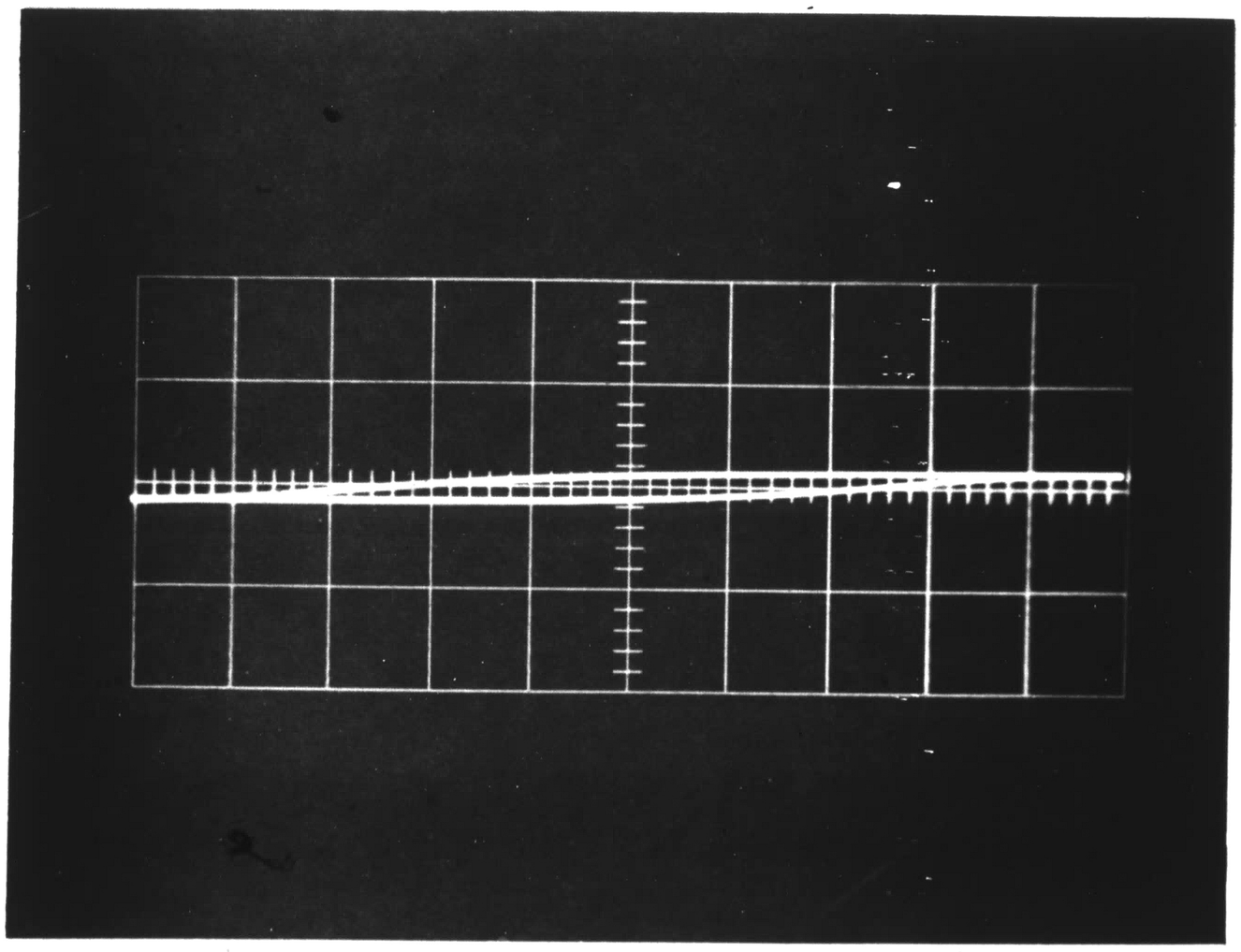

Figure 35. Hysteresis Loop of 11.3 w/o P Alloy Heat Treated 2 Hours at 400°C

REFERENCES

1. Brenner, Abner, "History of the Electroless Plating Process," Symposium on Electroless Nickel Plating, Special Technical Publication No. 265, A.S.T.M., Philadelphia, 1959, p. 5.

2. Brenner, A., and G. Riddell, "Deposition of Nickel and Cobalt by Chemical Reduction," Journal of Research of the National Bureau of Standards, Vol. 39, 1947, p. 394.

3. Brenner, A., et. al., "Electrodeposition of Alloys of Phosphorus with Nickel or Cobalt," Journal of Research of the National Bureau of Standards, Vol. 44, 1950, p. 117.

4. Koretsky, Herman, "Electrodeposited Magnetic Films: A Critical Survey," Proceedings of the First Australian Conference on Electrochemistry,(Friend, J.A. and F. Gutmann, eds.), Pergamon Press, New York, 1965, p. 418.

5. Zusmanovitch, G. G., "Effect of Heat Treatment on Hardness of Electroless Nickel Deposits," Metal Finishing, Vol. 59, 1961, pp. 52-54.

6. Metzger, W. H., "Characteristics of Deposits," Symposium on Electroless Nickel Plating, STP No. 265, ASTM, Phila., 1959, p. 16.

7. Goldenstein, A. W., et. al., "Structure of Chemically Deposited Nickel," Journal of the Electrochemical Society, Vol. 104, 1957, p. 104.

8. Brenner, A., Electrodeposition of Alloys Vol. II, Academic Press, New York, 1963, p. 471.

9. Graham, A. H., et. al., "Structure of Electroless Nickel," Journal of the Electrochemical Society, Vol. 109, 1962 pp. 1200-1201.

10. Hansen, M., Constitution of Binary Alloys, McGraw-Hill, New York, 1958, p. 692.

11. Bozorth, R. M., Ferromagnetism, D. Van Nostrand, New York, 1951, p. 322 - p. 251.

12. Brenner, op. cit., Reference No. 8, p. 119.

REFERENCES (cont'd)

13. Graham, A. H., et. al., "The Structure and Mechanical Properties of Electroless Nickel," Journal of the Electrochemical Society, Vol. 112, 1965, p. 401.

14. Hansen, op. cit.

15. Kotel'nikov, N. V., et. al., "The Magnetic Properties and Structure of Chemically Prepared Nickel Films," Soviet Physics-Doklady, Vol. 7, 1963, pp. 896-897.

16. Graham, op. cit., Reference No. 13, p. 402.

17. Nowotny, H., and E. Henglein, "X-Ray Investigation of the System Ni-P," Zeitschrift fuer Physikalische Chemie, Vol. B 40, 1938, pp. 281-284.

18. Pearson, W. B., Handbook of Lattice Spacings and Structures of Metals, Pergamon Press, New York, 1958, p. 781.

19. Goldenstein, op. cit. p. 107.

20. Graham, op. cit. Reference No. 13, p. 405.

21. Ibid, p. 406.

22. Brenner, op. cit. Reference No. 3, p. 118.

23. Kotel'nikov, op. cit.

24. Martius, U. M., "Ferromagnetism," Progress in Metal Physics Vol. 3, (B. Chalmers ed.), Macmillan, New York, 1961, p. 169.

25. Graham, op. cit., Reference No. 20.

26. Neel, L., "Effect of Thermal Fluctuations on the Magnetization of Small Particles," Comtes Rendus, Vol. 228, 1949, pp. 664-666.

27. Goldenstein, op. cit. p. 109.

28. Industrial Methods Manual, Section 4, Plating Solutions, New York, Bausch and Lomb: Catalog No. 33-29-06, pp. 21-25.

29. Crittenden, E. C., Jr., et. al., "Magnetization Hysteresis Loop Tracer for Long Specimens of Extremely Small Cross Section," The Review of Scientific Instruments, Vol. 22, 1951, pp. 872-877.

GENERAL REFERENCES

1. Brenner, A., Electrodeposition of Alloys, Vol. I and Vol. II, Academic Press, New York, 1963.

2. Bozorth, R. M., Ferromagnetism, D. Van Nostrand, New York, 1951.

3. Wert, C. A., and R. M. Thomson, Physics of Solids, McGraw-Hill, New York, 1964.

4. Cullity, B. D., Elements of X-Ray Diffraction, Addison-Wesley, Reading, Mass., 1956.

5. Azaroff, L. V., and M. J. Buerger, The Powder Method in X-Ray Crystallography, McGraw-Hill, New York, 1958.

APPENDIX A

Determination of Phosphorus in Nickel-Phosphorus Alloys

This is an adaptation of a Bausch and Lomb procedure for determination of phosphate in gold plating solutions[28].

The most useful range of a transmittance curve is approximately from 90% to 10%. The curve in question shown in Figure 36 was linear, as expected, on a semi-logarithmic plot. Therefore the sample size had to be adjusted to utilize the useful range of the curve which meant having 0.001 to 0.010 mg/ml P in step 10 below. The samples, as outlined in 5.2.2 weighed approximately 0.035 gm. Thus the method was as follows:

Reagents

Ammonium Molybdate Solution - Add 25 g $(NH_4)_6Mo_7O_2 \cdot 4H_2O$ to 1 liter volumetric flask. Add 300 ml H_2O. Add 500 ml 3:1 H_2SO_4 and make to volume with H_2O.

A.N.S.A. (1-Amino-2-Naphthol-4-Sulfonic Acid) - Add 97.5 ml 15% sodium bisulfite (15 g $NaHSO_3$ made to 100 ml with H_2O) to 100.0 mg A.N.S.A. in a beaker. Add 2.5 ml 20% sodium sulfite (5 g Na_2SO_3 made to 25 ml with H_2O), stir and filter. Store in dark bottle with maximum shelf life of two to four weeks.

Standard Phosphorus Solution - This solution should be prepared for the color development check given in step 11 below and as a standard but it must be remembered that the amount of phosphorus here will not be consistent with an equal amount in the alloy. Calibration will be necessary. Solution - Add 3.515 g

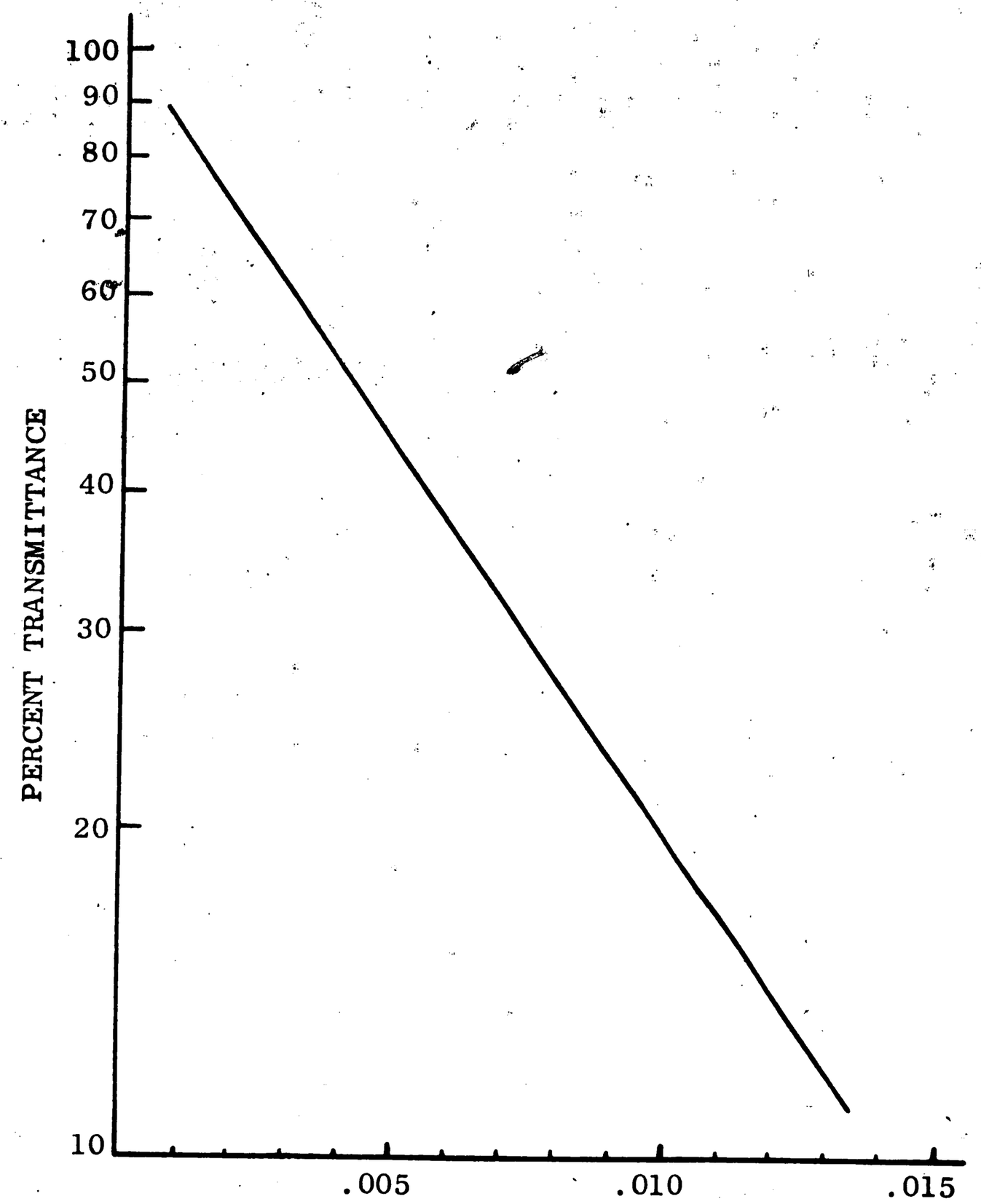

FIGURE 36 COLORIMETRIC DETERMINATION OF PHOSPHORUS IN NICKEL-PHOSPHORUS ALLOYS

of dried monobasic potassium phosphate (KH_2PO_4) to 1 liter volumetric flask and make to volume with H_2O. Transfer 25 ml to I liter volumetric flask and make to volume with H_2O. This solution contains 0.020 mg P/ml and a 25 ml aliquot when carried through steps 6-10 will have 0.005 mg P/ml.

Procedure

1. Place sample in 100 ml volumetric flask and add 10 ml

1:1 HNO_3.

2. Boil to expel brown fumes.

3. Cool and make to volume with H_2O.

4. Estimate mg/ml P from weight of sample and estimated w/o P by consideration of Figure 4.

5. Take aliquot containing 0.20 to 1.00 mg P and place in 100 ml volumetric flask.

Sample Calculation

wt. of sample	0.035 gm
x w/o P	0.12
	0.0042 gm P
	4.2 mg P
diluted to 100 ml	0.042 mg/ml P
15 ml aliquot	0.63 mg P
step 10 below	0.0063 mg/ml P

6. Add 1 drop 0.1% phenolphthalein and then NH_4OH dropwise to appearance of pink hue.

7. Add 1 ml concentrated H_2SO_4.

8. Add 10 ml of molybdate solution and mix.

9. Add 4 ml of A.N.S.A. and mix.

10. Make to volume with H_2O and mix.

11. Set 100% transmittance on spectrophotometer at 650 mμ using reagent blank which is distilled water carried thru steps 6 to 10.

12. Determine color development completion with standard carried thru steps 6 to 10; usually 15 minutes is sufficient.

13. Read percent transmittance of samples after color development is complete.

14. Read mg/ml P from transmittance curve.

15. Determine % P in original sample.

Sample Calculation

0.0063 mg/ml P in 100 ml = 0.63 mg P

$$0.63 \text{ mg P} \times \frac{100 \text{ ml (original volume)}}{15 \text{ ml (aliquot taken)}} = 4.2 \text{ mg P}$$

$$\frac{4.2 \text{ mg P}}{35 \text{ mg alloy}} \times 100\% = 12\% \text{ P}$$

APPENDIX B

Hysteresis Loop Tracer

The instrument is shown in Figure 5, Figure 6, and Figure 7.

Specifications

Helmholtz Coil - two series connected field coils of 450 turns each of no. 12 AWG enameled copper wire, mean radius and separation = 11 cm.

Pickup Coil - 9000 turns of no. 42 AWG enameled copper wire, core dimensions 4 cm x 0.15 cm.

Neutralizing Coil - 12000 turns, otherwise identical to pick up coil.

Oscilloscope - Tektronix 545A with Type D Plug-In Unit Pre-amplifier.

Integrator-Amplifier - Tektronix Type O operational amplifier plug-in unit with Type 132 plug-in unit power supply.

Power Supply - was constructed by author from schematic of Figure 7. Note: 52 UF capacitor shown provides correct resonance for circuit. A 54 UF capacitor was used because of availability but limits output to field coils to 15 amps.

Calibrating Instrument - Bell Model 240 Gaussmeter.

Theory[29]

The AC loop tracer is commonly used for magnetic measurement on film specimens such as those obtained by electrodeposition where a large number of samples are involved and a very precise measurement is not required. The instrument is not as precise as static DC

loop plotters but has the advantage of convenience and speed. The accuracy, which can reasonably be taken to be ± 5%, is dependent primarily upon two factors; reproducibility of reading the oscilloscope and the accuracy of the calibrating instrument.

Theoretically the unit may be powered by an AC supply at any low frequency. In practice, however, very low frequencies result in excessive electronic tube noise and higher frequencies tend to create eddy currents in the sample so that 60 cycles becomes a good compromise. Since it is readily available there seems no reason to consider any other frequency.

A theoretical Helmholtz coil has two series connected coils of infinitesimally small cross section whose mean separation is equal to the mean radius. This produces a very uniform internal field which may be calculated from an equation. Since a theoretical coil cannot be constructed and the equation does not apply completely to the actual coil, the field must be calibrated to give more accurate values. The two values are, however, comparable.

The field coils must be rigidly braced and preferably coated with epoxy to prevent vibration but not so as to aggravate the heat dissipation problem. The internal field should be electrostatically shielded from the field coils by surrounding the I.D. of the latter with a grounded aluminum foil.

The pick up coil, into which the sample is placed, is located in the geometric center of the Helmholtz coil. With no sample in the pick up coil and under an applied field, a relatively large voltage, in comparison to with the sample, is induced in the pick up coil due

to air coupling between it and the field coils. In order to cancel this voltage it is necessary to employ a dimensionally equivalent neutralizing coil which is connected in series and wound in opposition creating a voltage opposite in phase and magnitude. Because it is difficult to make both coils identical, complete cancellation is not obtained. Final cancellation is achieved by adjusting the variable inductance designed into the instrument by allowing the neutralizing coil freedom of movement while the pick up coil remains fixed and insertion of a source of eddy currents in the form of a long strip of copper which also has freedom of movement.

Now, with a sample in place, the pick up coil becomes a sample-cored transformer whose induced voltage is proportional to d(B-H)/dt times A, time rate of change of magnetization times cross sectional area of sample, which is fed into an integrator and then to the vertical drive of the oscilloscope. The voltage across the 0.5 ohm resistor seen in the schematic of Figure 7 is proportional to the current supplied to the Helmholtz coil which is in turn linearly proportional to the field generated; defined as H. This is fed to the horizontal drive of the scope. The total result is a hysteresis loop displayed as (B-H) versus H.

In this case we are determining Hci or intrinsic coercive force which is the attribute obtained when the hysteresis curve is plotted as (B-H) versus H rather than B versus H which gives the commonly considered coercive force. Hci is the field required to make (B-H) equal zero. There is some confusion in the literature from data being presented as coercive force when actually intrinsic coercive force has

been measured. Hci is always greater than Hc.

Operation

The oscilloscope and accessories are turned on and allowed to warm up sufficiently. When performing measurements continuously over a period of days it is advisable to leave the scope on overnight to gain the maximum stability.

With no sample and under an applied field a trace is placed on the scope. Most generally it will be an oval loop. The loop is flattened into a line by adjusting the copper strip's position. The line trace is next made horizontal by adjusting the position of the neutralizing coil. The line is set to some convenient length by adjusting the variable horizontal knob on the scope. In this investigation it was found that all specimens could be completely saturated with a field which required 5 amps AC to generate. Therefore the horizontal trace on the scope was set to show full scale deflection of 50 units at 5 amps AC field current.

With field on, the sample is placed in the pick up coil producing a hysteresis loop which must be centered on the scope using the appropriate controls. The size of the loop may be varied or the sensitivity changed by adjustment of the gain of the Type D (or other) preamplifier and/or the appropriate R and C settings on the integrator. Readings should be made at consistent settings as far as practicable. Coercive force measurements are unaffected by these adjustments except where concerned with reading error.

The intrinsic coercive force may now be read directly from the scope by noting the horizontal deflection of the loop. As an

example consider that it is 20 divisions. This corresponds to 2 amps AC since the full scale of 50 divisions was set at 5 amps AC. Thus Hci may be read from the calibration curve showing field current in AC amps versus field strength in oersteds.

M_s, saturation magnetization, and M_r, remanent magnetization, may also be determined from the oscilloscope display but require more sophisticated calibration and calculation. Since coercive force is the parameter of most significance in this investigation, it was decided to observe M only in a semi-quantitative manner and not determine explicit values. If the reader is interested in actual determination of M, reference should be made to the article by Crittenden[29] and the instruction manual for the Tektronix Type O accessory.

VITA

Jim Riley Goodin was born August 8, 1935 in Shawnee, Oklahoma. He graduated from Shawnee High School in 1954 and attended Oklahoma Baptist University in the same city through 1959, receiving the degree of Bachelor of Arts in Chemistry.

In 1960 he joined the engineering organization of the Oklahoma City Works of the Western Electric Company. During his tenure there he was assigned to the engineering laboratories and subsequently as materials engineer.

In 1965 came a transfer to the Engineering Research Center at Princeton, New Jersey and an assignment to the Lehigh Master's Program under the joint sponsorship of Lehigh University and Western Electric. Through the University he pursued the degree of Master of Science in Metallurgical Engineering. In addition to the program he was assigned to the metal deposition group at the center and worked on electro and electroless deposition studies.